Proposal of a mix design method for low cement fiber reinforced concrete

Mohd Nabil Eid

A Thesis submitted to the University of Ottawa
in partial Fulfillment of the requirements for the

MASTER OF APPLIED SCIENCE

in Civil Engineering

Department of Civil Engineering

Faculty of Engineering

University of Ottawa

Abstract

Concrete, the second most used material in the world, presents great performance and economic benefits. Yet, it is often characterized by a brittle behaviour, low tensile strength, and toughness. Fibers are usually added to concrete to counteract its brittle behaviour, increasing ductility and toughness, controlling crack propagation and delaying concrete failure. However, their addition significantly worsens the fresh state performance of the material. To improve fresh state of the so-called *Fiber Reinforced Concrete* (FRC), conventional mix-design methods recommend the use of high paste content, which results in a significant increase of Portland cement (PC) content and raises the carbon footprint of the material. The latter is responsible for 8% of the global annual carbon dioxide (CO_2) anthropogenic emissions. Given the current worldwide concerns on global warming, the construction industry is in a need to lessen the demand, and thus production of PC. Recent studies have been focusing on the use of advanced mix-design techniques (i.e. particle packing models- PPMs) along with Inert Fillers (IF) as an alternative to reduce PC content in concrete. However, the latter was not applied to conventional FRC. In this work, advanced mix design techniques (i.e. PPMs) are used to overcome the aforementioned issues and mix-proportion eco-efficient FRC with low cement content (< 300 kg/m^3). Fresh (i.e. VeBe time, slump, rheological behaviour) and hardened (i.e. compressive strength, and flexural behaviour) state tests were performed on the proposed mixtures and compared with control high PC content (375 kg/m^3) FRC mixes. Results show that PPM designed mixes presented higher minimum torque (yield stress) but quite comparable apparent viscositiy when compared to conventionally designed mixtures. Moreover, the flowability (i.e. VeBe time, and slump) tends to decrease as fiber content, length, and/or as the amount of fillers increase in the mixtures. In addition, PPM mixes exhibited a shear thinning behaviour following the Herschel-Bulkley model, which enables the design of FRC PPM mix-proportioned mixtures for applications requiring high torque regimes such as vibrated and/or pumped concrete. Finally, results show that the use of PPMs to mix proportion eco-efficient low cement FRC mixtures produced improved hardened (i.e. compressive strength, and flexural performance) state behaviour with lower environmental impact than conventional ACI designed FRC mixtures.

Keywords: mix design; sustainability; particle packing models; fiber reinforced concrete; flowability; VeBe time; rheology; binder intensity; Interparticle Separation Distance; Maximum Paste Thickness; Fiber Factor.

Acknowledgements

First and foremost, I am thankful to God for the opportunity I was given to conclude a Master of Applied science in Civil Engineering at University of Ottawa, which was a dream, and a goal set well over five years ago.

I would like to acknowledge, and express my deepest gratitude to my supervisor Dr. Leandro Sanchez, who not only provided me with a great amount of knowledge in concrete, but also taught me to be patient and to always look for ways to improve my skillset weather in research, or in life. Moreover, Dr. Sanchez has also become a friend, who believed in my potential, with his effort and availability. Finally, he taught me how to work in a collaborative team, work ethic and gave me the opportunity to coordinate our research group activities over a full term session.

The support of my family, parents, brothers and sisters during the past two years, in which their encouragement was my pillar to stand on whenever doubt slowed down my work pace. As well as my team-mates from our research group, who was there to help in the laboratory, as well as with their constructing criticism during presentations, which all was one factor that brought the success of this project.

I would also like to be thankful for the Civil Engineering department personnel's, who gave me the opportunity to work as a teacher assistant during my graduate studies, which significantly developed my mentoring skills, as well as their efforts to always find a solution when logistical difficulties arose during this project.

I'm also thankful for the help of the lab technicians at University of Ottawa, Muslim Majeed, and Gamal Elnabelsya, for teaching me how to perform the daily tasks while diligently ensuring that safety guidelines are always followed.

Last but not least, I would like to be extremely thankful for my supervisors at best buy, my part time job during my graduate studies, who always believed in my ability to successfully finish this project, and always accommodated my time availabilities.

Table of Contents

List of Figures

List of Tables

List of Symbols/Abbreviations

ACI	American Concrete Institute
a_i	Apparent Volume of the i^{th} size particle in a Monodisperse System
BC	Binder Content
Bi	Binder Intensity
$CaCo_3$	Limestone
CaO	Lime
Co	Carbon Monoxide
CO_2	Carbon Dioxide
CPFT	Cumulative (Volume) Percent Finer Than D
CPM	Compressive Packing Model
CSA	Canadian Standard Association
D	Maximum Aggregate Size
Deq-fibers	Fiber Equivalent Diameter
d_f	Fiber Diameter
d_o	Particle Diameter
dv	Fiber Volumetric Diameter
F_{600}^d	Residual Strength at net deflection of L/600
F_{150}^d	Residual Strength at net deflection of L/150
f'c	Concrete Compressive Strength
f_{cc}	Concrete Flexural Strength
FMF	Fiber Matrix Factor
FRC	Fiber Reinforced Concrete
He	Helium Gas
IF	Inert Fillers
IPS	Interparticle Spacing
K	Empirical Factor
L_f	Fiber Length
MPT	Maximum Paste Thickness
MSF	Matrix Spacing Factor
n	Flow Behaviour Factor
P	Performance Requirement
P_{600}^d	Residual Load at net deflection of L/600
P_{150}^d	Residual Load at net deflection of L/150
PBD	Performance Based Design
PC	Portland Cement
PF	Packing Factor
PP	Polypropylene Fibers
PPMs	Particle Packing Models
PSD	Particle Size Distribution
P_{of}	Pore Fraction
P_{ofc}	Pore of Aggregate Fraction assuming the densest Packing
q	Distribution coefficient
S	Steel Fibers
SCC	Self Compacting Concrete
SCMs	Supplementary Cementitious Materials
SSA	Specific Surface Area
UHPFRC	Ultra high-Performance Fiber Reinforced Concrete
UTM	Universal Testing Machine
V1	Fraction of Small Particles Solid Volume
V2	Fraction of Large Particles Solid Volume
V_a	Apparent Volume
V_{ai}	Apparent Volume of the Mixture with n Particle Sizes
Vf	Volume of fibers

Vs	Volume of Solids
VSA	Volume Surface Area
VSA_c	Calculated Volume surface Area of Aggregate Fraction
V_{sc}	Volumetric Aggregate Solid Fraction
W/C	Water to Cement Ratio
XRF	X-ray fluorescence
x_i	Mass Fraction of i^{th} Size Particle
ϕ	Packing Density
ψ	Sphericity
τ	Torque
τ_o	Yield Torque
γ	Speed of Rotation
γaggregate	Specific Weight of Aggregates
γfiber	Specific Weight of Fibers

Chapter One: Introduction

1.1 OVERVIEW

Concrete is the second most used material in the world after water. It is used in a variety of construction projects worldwide from sidewalks and culverts, to high rise tower buildings and bridges. Concrete displays interesting performance (high strength and durability in the hardened state, flowability and capacity of molding any geometry in the fresh state, etc.) at a relatively low cost when compared to other building materials such as steel or timber. Mainly, concrete consists of an aggregate skeleton comprised of different sizes and shapes, and paste filling the volume of the skeleton's interstices. The paste is usually made up of cementing materials and water; it binds the aggregates together in the hardened state, which generates a construction material with suitable mechanical properties.

Cementing materials, especially Portland cement (PC), are the most expensive components of concrete, and their production imposes high environmental impacts. PC production is responsible for about 8% of the anthropogenic annual CO_2 emissions (Andrew, 2017). Moreover, the building materials sector ranks as the third largest CO_2 emitting industrial sector worldwide (Rui Yu et al., 2017). Furthermore, global PC production has increased by more than 30-fold since 1950 and almost 4-fold since 1990. The latter has largely been due to the rapid development in China where PC production has grown by a factor of 12 (73% after 1990) (Andrew, 2017). Studies have shown that the production of one ton of PC produces approximately one ton of CO_2 (Rui Yu et al., 2017). There are two aspects of cement production that result in CO_2 emissions; the first is the chemical reaction involved in the production of the clinker (main PC component), where carbonates (largely limestone, $CaCO_3$) are decomposed into oxides (mostly lime, CaO) and CO_2 by the addition of heat as described by the following chemical reaction as shown in Equation 1.1. Recent studies showed this process contributes to about 5% of total anthropogenic CO_2 emissions, excluding land use change.

$$CaCo_3 \rightarrow \text{CaO} + \text{CO} \qquad \text{Equation 1.1}$$

The second source of emissions is the combustion of fossil fuel to generate significant energy required to heat the raw materials up to well over 1000°C. The latter "energy" emissions including those purchased from electrical sources, adds a further 60% on top of the process emissions (Andrew, 2017). Figures 1.1 and 1.2 displays the worldwide production volumes of cement and CO_2 emissions, respectively.

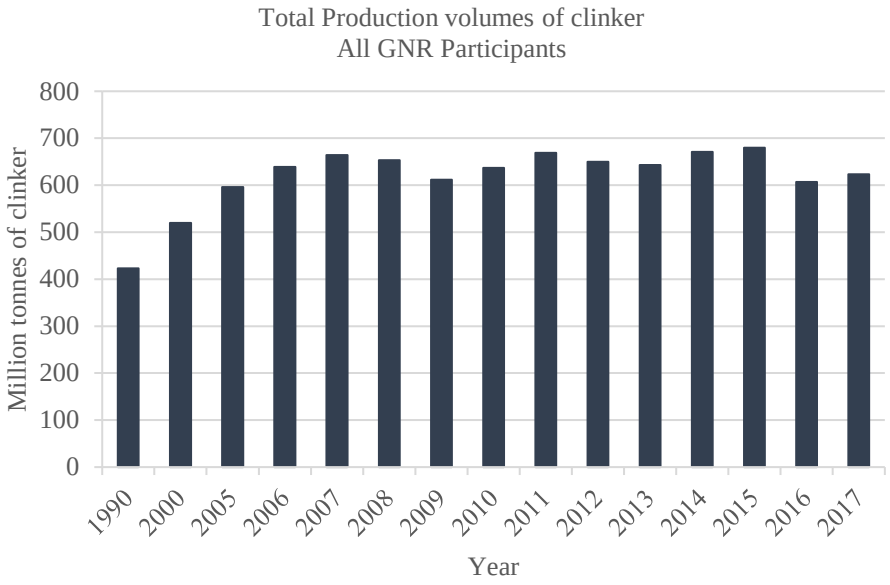

Figure 1.1 Worldwide production volume of cement from the year 1990 to 2017.

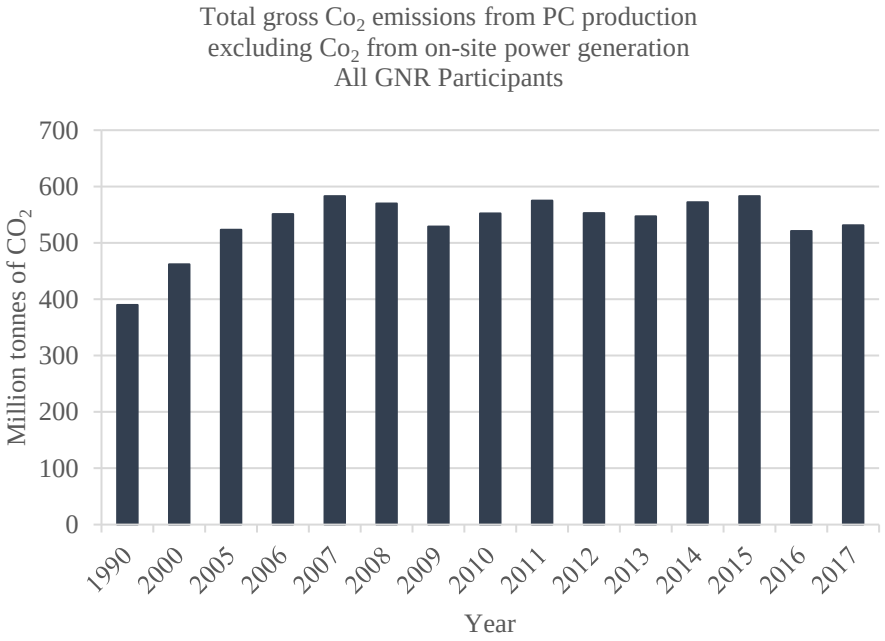

Figure 1.2 Worldwide production volume of CO2 emissions from the year 1990 to 2017.

Plain concrete is a brittle material in the hardened state, with low tensile strength, ductility, and toughness. Fibers are usually added to concrete to counteract these problems. Fibers are often divided into “micro” and “macro” fibers; micro fibers are used to improve strength and ultimate capacity of concrete although macro fibers are selected to

control “concrete cracking”, increasing strain capacity (i.e. ductility) and toughness (i.e. amount of energy released) of the material before failure (Bentur & Sidney, 2007).

Currently, there are 200,000 metric tons of fibers being used as reinforcement in concrete; the main application of fibers in the construction industry is in precast members, tunnel linings, airway pavements and sidewalks (Nemkumar Banthia, Bindiganavile, Jones, & Novak, 2014; Nemkumar Banthia, Zanotti, & Sappakittipakorn, 2014). Although fiber reinforced concrete (FRC) presents numerous advantages in the hardened state, the addition of fibers significantly worsens the fresh state behaviour of the material. Difficulties in mixing, transporting, handling and placing are conditions that may lead to poor compaction and thus compromising properties in the hardened state (Bentur & Sidney, 2007; Figueiredo & Ceccato, 2015; Guerini, Conforti, Plizzari, & Kawashima, 2018). To account for flowability issues in the fresh state, conventional mix-design methods often require high paste content for FRC, which results in significant increase of PC content (i.e. 400 to 500 kg/m^3) and raises the carbon footprint of the material (Labib, 2018; Wafa, 1990). Recent studies have been focusing on three main approaches to reduce the carbon footprint of concrete; the first approach consists of the use of supplementary cementitious materials (SCMS) and/or inert fillers (IF) as a partial replacement of PC; the second one focuses on more efficient technologies to produce cement releasing less CO_2; and the third approach consists of optimizing PC efficiency in concrete mixtures through the use of advanced mix-design techniques (i.e. particle packing models- PPMs) (Dadsetan, Grazia, & Sanchez, 2017; T. de Grazia, F. M. Sanchez, C. O. Romano, & G. Pileggi, 2019). Despite the widely known efficiency of SCMs (i.e. fly ash, blast furnace slag, silica fume, etc.) as a replacement of PC, since they improve concrete performance, durability, and sustainability, their available supply does not increase as the same rate of PC demand (Dadsetan et al., 2017; Damineli, B. L. & John, 2012). On the other hand, studies showed that IF can be used as a partial replacement and/or an addition to PC, resulting in benefits to concrete properties and reducing its environmental impact (Dadsetan et al., 2017; Varhen, Dilonardo, de Oliveira Romano, Pileggi, & de Figueiredo, 2016). Likewise, the latter approach cannot match the rapid annual growth of PC demand. Finally, it has been found that the third approach is quite effective in reducing PC content in concrete mixtures (by more than 50% in some cases) while keeping and/or improving their mechanical properties when compared to mixes proportioned through conventional methods (Fennis & Walraven, 2012; Yousuf, Sanchez, & Shammeh, 2019). However, there is a lack of studies regarding the best way to reduce PC content in conventional FRC mixtures, along with a lack of understanding on how to implement PPMs to proportion FRC

mixtures, and how they might affect the fresh (i.e. VeBe time, slump, and rheology) and hardened (i.e. compressive, and flexural strength) properties of FRC.

1.2 RESEARCH OBJECTIVES

The main objective of this research is to evaluate the suitability of PPMs to proportion conventional FRC with reduced amount of PC (i.e. $\leq$ 300 kg/m^3) and appraise their impact on the fresh and hardened state properties of the material. In this research program, different types of eco-efficient FRC mixtures were mix-proportioned through PPMs containing different types of fibers (i.e. steel, and polypropylene), fiber contents (i.e. 0.5%, and 1.0% Vf) and lengths (i.e. 38, and 50 mm). It is worth noting that eco-efficient FRC is defined as conventional FRC with reduced amounts of PC (i.e. 320 kg/m3 or less, which is the minimum content recommended by the American Concrete Institute – ACI for concrete exposed to the environment) with fresh and hardened states performance in accordance to the project requirements.These mixtures were evaluated in the fresh (i.e. VeBe time, slump, and rheometry) and hardened (i.e. compressive strength, and flexural performance) states. Moreover, conventional FRC mixtures were mix-proportioned through conventional techniques (i.e. ACI - absolute volume method) containing similar fiber types, contents, and lengths. Comparisons among the distinct properties from PPM and ACI designed mixtures were then conducted and final considerations on the use of PPMs to proportion eco-efficient FRC mixtures with suitable properties are then performed.

1.3 THESIS ORGANIZATION

This Thesis is divided into four chapters. Chapter 1 discusses on the current concerns related to concrete's carbon footprint, and high PC content often used for FRC mixtures. Furthermore, Chapter 1 also displays the Thesis main objectives and overall organization.

Chapter 2 presents a detailed literature review on the use of PPMs as a novel mix-proportioning technique to produce eco-efficient FRC with suitable properties in the fresh and hardened states. This section discusses the following topics: mix-design methods, PPMs, mobility parameters, limestone fillers effect, binder efficiency, FRC, fresh state behaviour of FRC, fiber effects on packing density, and hardened state behaviour of FRC.

Chapter 3 consists of a journal paper which evaluates the effect of using a continuous PPM (i.e. Alfred model) to mix-proportion distinct FRC mixtures with low amounts of PC and suitable performance in the fresh and hardened states.

Chapter 4 brings the conclusion obtained throughout this project and proposes suggestions for future research in the area.

CHAPTER TWO: LITERATURE REVIEW

2.1 MIX DESIGN METHODS

The process of selecting the distinct ingredients (and their proportions) to meet required properties and criteria for concrete mixtures is the so-called mix-proportioning or mix-design. The required criteria may include fresh (i.e. consistency, flowability, workability, etc.), and hardened state properties (i.e. compressive and tensile strength, stiffness, etc.) along with durability requirements. A properly proportioned concrete mixture should present suitable fresh and hardened performance, besides being eco-efficient (low carbon footprint) and economic.

There are a wide range of mix-proportioning techniques that might be selected to proportion conventional concrete. Amongst those, one may distinguish two types of categories: conventional and or engineering approaches (e.g. absolute volume method or ACI method) and scientific approaches (e.g. Particle Packing Models – PPMs).

2.1.1 ACI METHOD

The ACI mix-design method is a quite simple technique and likely the most commonly used method in North America. It is governed by the selection of fresh (i.e. consistency through the slump value) and hardened state (compressive strength and durability as a function of the water-to-cement ratio) properties. Moreover, the exposure condition is an important factor that must be considered as it defines the maximum water-to-cement ratio, minimum compressive strength, and air content of the material. However, this approach often results in non-eco-friendly mixtures with moderate to high amounts of PC (e.g. 350 to 450 kg/m^3). Furthermore, this method disregards important factors of the mix such as the particle size distribution (PSD) of the binder and aggregates selected for use, along with the lithotype, shape, and texture of coarse and fine aggregates. These parameters play an important role on the fresh (e.g. flowability) and hardened (e.g. stiffness, durability, etc.) state properties of concrete (Komastka, Kerkhoff, & Panarese, 2003; Neville & Brooks, 2010). Finally, ACI method only provides empirical approaches for the consideration of new components such as fibers in the mixture, without accounting for the physical properties of these inclusions.

2.1.2 PARTICLE PACKING MODELS

It is widely known that concrete can be considered as a two-phase material, consisting roughly of an aggregate skeleton embedded into a cementitious matrix. The voids within the aggregate skeleton determines the minimum cement paste content required to first bind all the particles together, and second create a separation layer which induces a certain flowability. Therefore, the selection of an optimized aggregates PSD is quite important, leading to systems with high packing density, low porosity and embodied energy (Fennis & Walraven, 2012; Mangulkar & Jamkar, 2013). Packing density is defined as the ratio of the solid volume of the aggregate particles to the bulk volume occupied by the aggregates, given by Equation 2.1.

$$Packing\ density\ (\phi) = \frac{Solid\ volume}{Total\ volume} \qquad Equation\ 2.1$$

Where "Solid volume" is the volume of solids, and "Total volume" is the volume of solids plus volume of voids as shown in Figure 2.1.

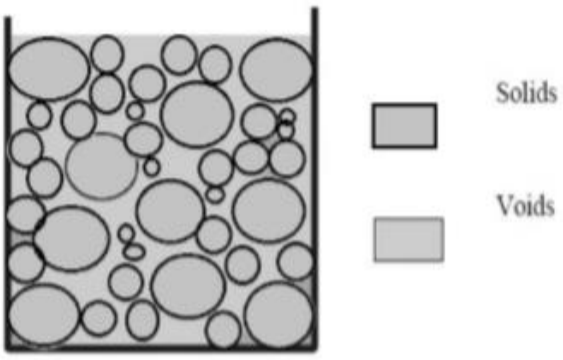

Figure 2.1 Definition of packing density adopted from (Mangulkar & Jamkar, 2013).

Packing density is inversely proportional to the voids fraction. It may be affected by a number of factors; yet, the most important parameters are: the size, shape, and volume of the particles, along with the distances among them and their electrostatic interactions (Grazia, 2018; Kawashima, 2012).

PPMs are numerical based models that can be used to optimize the grading of the aggregates, where finer particles fill the volume between coarser ones without disturbing their packing. These finer particles create another level of voids that can be next filled by even finer particles, resulting in a system with high packing density and low porosity (Fennis

& Walraven, 2012; Kumar & Santhanam, 2003; Mangulkar & Jamkar, 2013). However, when a finer particle is too large to fill the void of adjacent coarser particles, it causes disturbance to their packing resulting in a system with increased porosity. This phenomenon is known as the loosening effect and is illustrated in Figure 2.2. On the other hand, once an isolated coarser particle is in the vicinity of fine particles, it disturbs their packing resulting in a system with increased porosity, which is known as the so-called Wall effect as illustrated in Figure 2.2 (Fennis & Walraven, 2012; Mangulkar & Jamkar, 2013).

Figure 2.2 Wall Effect and Loosening Effect

The packing density of granular systems changes as a function of the casting process. When particles are placed one by one, the maximum packing density is achieved easily, and is called the virtual packing density. On the other hand, in real casting scenarios, the aggregates are placed randomly with different energies, resulting in a much lower packing density than the virtual packing density (Kawashima, 2012). Normally, the voids formed between the aggregates are filled with cement paste; therefore, reducing the system porosity results in a lower need for cement paste. In 1930, Westman and Hugill developed an algorithm through the Equation set 2.2 to calculate the *packing factor* (PF) based on packing theories. PF is defined as the relationship between compacted bulk density and loose bulk density of aggregates, which can be increased with the raise of fine and coarse aggregates in the mix (Funk & Dinger, 1994; Vogt, 2010).

$$\begin{gathered} Va1 = a1x13 \\ Va2 = x1 + a2x2 \\ Va3 = x1 + x2 + a3x3 \\ \dots \\ Vai = \sum_{j=1}^{i-1} xj + aixi \end{gathered} \qquad Equation\ 2.2$$

Where ai is the apparent volume of the i^{th} size particle in a monodisperse system, x_i is the mass fraction of i^{th} size particle, V_{ai} is the apparent volume of the mixture with n particle sizes, n is the number of particle sizes.

It is known that the maximum apparent volume (Va) given in Equation 2.3 is directly proportional to the porosity and inversely proportional to the PF (Funk & Dinger, 1994).

$$Va = \frac{1}{PF} \qquad Equation\ 2.3$$

Fine and coarse aggregates are in reality non-spherical particles; however, considering monodisperse spherical particles filling a bucket of a given volume, it would result in a total of approximately 25% of empty spaces. This results in a packing density of around 75%, which is only a theoretical value. In real scenarios, it would result in packing density values ranging from 60% to 64%. Thus, monodisperse systems have a porosity equal to 40% for maximum packing. The porosity of real distributions can be calculated with the modified Westman and Hugill algorithm given in Equation 2.4 (Funk & Dinger, 1994).

$$Porosity\ (\%) = \left(1 - \frac{1}{Va}\right) * 40\% \qquad Equation\ 2.4$$

PPMs can be generally divided into two groups, discrete and continuous. Discrete models (also known as gap-graded systems) are combinations of "n" discrete size classes of particles where each particle class pack to its maximum packing density in the available volume. The second group, continuous PPMs, assumes that all possible size classes are present in the mixture with no gaps within the total PSD. Moreover, continuous PPMs considers a "similarity condition" of the particle's adjacent environment regardless of the particle size (Fennis & Walraven, 2012; Mangulkar & Jamkar, 2013).

Discrete models aim to achieve the maximum packing density by adding the maximum amount of coarse aggregate in a specified volume and then filling in the voids with finer particles. One of the first discrete models developed was the Furnas model for binary mixtures. This model is only valid whenever the fine particle size was much smaller compared to the coarse particle size. If the ratio between the fine and coarse aggregate sizes is close to one, there can be two negative interaction effects: wall and loosening effects as shown in Figure 2.2.

Probably the first continuous models was brought by Fuller and Thompson in 1907 (Fuller, W.B.; Thompson, 1907). In the "Fuller-Thompson" model, the "ideal" grading curve is the one that maximizes packing density according to Equation 2.5.

$$CPFT = (d/D)^n * 100 \qquad Equation\ 2.5$$

Where CPFT is the cumulative percent finer than d, d is the given particle size, D is the maximum particle size and n was found to be optimal from 0.45 to 0.5 (Kumar & Santhanam, 2003; Mangulkar & Jamkar, 2013).

Andreasen (1930) followed the previous work developed by Fuller and Thompson, and after some experimental testing and modelling, the author developed an "ideal" particle packing curve according to Equation 2.6, where it was assumed that the smallest particle size would be infinitesimally small.

$$CPFT = (d/D)^q * 100 \qquad Equation\ 2.6$$

Where CPFT is the cumulative percent finer than d, d is the given particle size, D is the maximum particle size and q is the distribution factor. Andreasen suggested that the optimal q factor should range between 0.33 and 0.50 (Kumar & Santhanam, 2003; Mangulkar & Jamkar, 2013). Moreover, according to Andreasen an ideal grading curve occurs where there is a similarity in the particle's distribution and arrangement irrespective of the aggregate size, the so-called granulation image as illustrated in Figure 2.3 (Vogt, 2010).

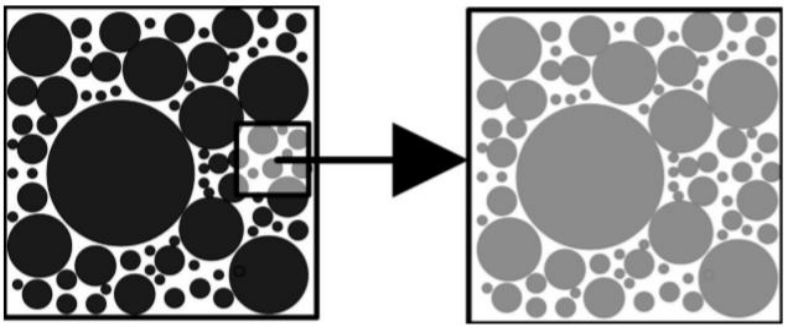

Figure 2.3 illustration of the similarity condition (Vogt, 2010).

In 1980, Funk and Dinger realized that any real PSD must account for the smallest particle size and modified the Andreasen Equation as given by Equation 2.7, defined as the Alfred or the modified Andreasen model (Funk & Dinger, 1994; Mangulkar & Jamkar, 2013). The q-factor (ranging from 0.21-0.37) in Alfred's model defines the fine/course

aggregate ratio and is selected based on workability requirements (Fennis & Walraven, 2012; Grazia, 2018; Mangulkar & Jamkar, 2013). After some experimental work, the authors suggested that the densest packing could be achieved with a q factor equal to 0.37, which would likely bring benefits to the short and long-term hardened state properties of concrete along with decreasing the binder content of the mixture. Otherwise, it has been found that whether the distribution factor raises above 0.37, the porosity of the system rises instantly. It is worth noting that low q-factor yields higher fines content in the mixture while high q-values yields higher coarse content. Q factors ranging between 0.21 to 0.23 are suggested for SCC, whereas values of about 0.25-0.3 are often used for for HPC. Finally, it is suggested that q factors greater than 0.32 be selected for roller-compacted concrete (Mangulkar & Jamkar, 2013).

$$CPFT = \left(\frac{d - do}{D - do}\right)^{q} * 100 \qquad Equation\ 2.7$$

Where CPFT is the cumulative (volume) percent finer than d, d is the given particle diameter, d*o* is the smallest particle diameter, D is the largest particle diameter, and q is the distribution factor.

The difference between q-factors of 0.21, and 0.37 are illustrated in Figure 2.4.

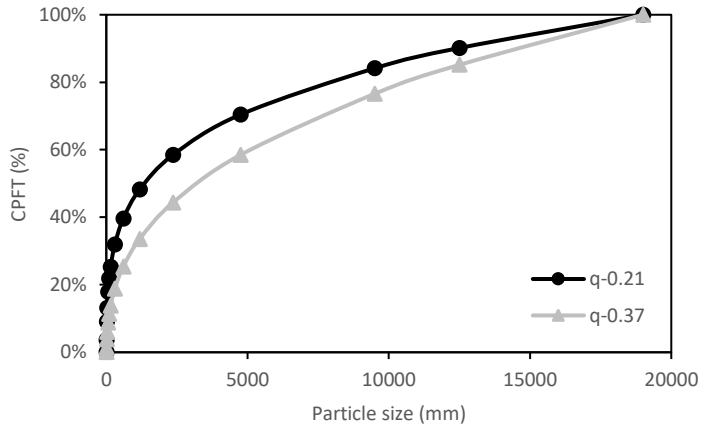

Figure 2.4 Particle size distribution of different q-factors using Alfred model.

Figure 2.5 illustrates the effect of the q distribution factor on the porosity of different systems, based on the applying the Westman and Hugill concepts to Alfred model.

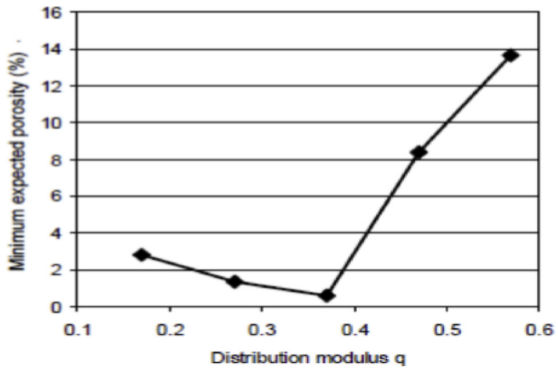

Figure 2.5 Relationship between expected porosity and q-factor.

One of the drawbacks of using continuous PPMs (i.e. Alfred model) is that it only accounts for the dry material (i.e. water and PC hydration are disregarded in the design). Furthermore, aggregates characteristics such as shape, texture, and lithotype are only accounted indirectly (through changes in the distribution factor). Finally, there are no variable to quantify and or forecast the fresh properties of concrete mixtures designed through PPMs. Therefore, other techniques studying the mobility among the particles throughout the whole PSD of the system is required to understand the fresh state properties of concrete mixtures designed through PPMs.

Concrete in the fresh state can be considered as a two phase material consisting of a cement paste phase governed by surface forces, and aggregates governed by mass and gravitational forces (de Oliveira, Ivone R.; Studart, Pileggi, & Pandolfelli, 2000; Innocentini, Pileggi, Ramal, & Pandolfelli, 2003), with particle sizes ranging from (0-150μm) for the former and larger than 150 μm for the latter (Grazia, 2018). The cement paste constituents are governed by surface forces, where in the aggregate phase interaction is governed by mass and gravitational forces(de Oliveira, Ivone R.; Studart et al., 2000). Therefore, understanding concrete in the fresh state requires clear definition of each phase separately. Previous research shows that the Interparticle Separation Distance (IPS) and Maximum Paste Thickness presented in Figure 2.6 are two mobility parameters that are essential to understanding the concrete fresh state behaviour (T. de Grazia et al., 2019). The IPS measures the mean distance separating particles in the cement paste, which is given in Equation 2.8. IPS is calculated assuming no particle agglomeration and that a part of the fluid in the paste fills the voids and covers the surface of particles, where the remaining fluid builds up the separating layer of particles.

$$IPS = \frac{2}{VSA}\left[\frac{1}{Vs} - \frac{1}{(1 - Pof)}\right] \qquad Equation\ 2.8$$

Where IPS is the interparticle separation distance, VSA is the volumetric surface area of powder (m^2/cm^3), Vs is the volumetric solid fraction of powder, and P_{of} is the powder pore fraction at maximum packing condition.

Otherwise, the maximum separating distance of particles within the aggregates can be calculated through the MPT parameter given in Equation 2.9 (Funk & Dinger, 1994; Ortega, Pileggi, Studart, & Pandolfelli, 2002).

$$MPT = \frac{2}{VSAc}\left[\frac{1}{Vsc} - \frac{1}{(1 - Pofc)}\right] \qquad Equation\ 2.9$$

Where MPT is the distance between aggregates, VSAc is the volumetric surface area of aggregate fraction, Vsc is the volumetric solid fraction of aggregate fraction, and P_{of} is the aggregate pore fraction at maximum packing condition. Research shows that flowability of concrete mixtures increase as the IPS and MPT increase. The latter is a result of a decrease of friction among the particles without changing the water content. Finally, these two mobility parameters are directly proportional to the concrete microstructure (e.g. permeability) as shown in Figure 2.6. De Grazia et al. (2019) used Alfred model to mix proportion the so-called Low Cement Concrete (LCC). The author performed rheological testing and correlated the mixing energy to the IPS, and MPT mobility parameters. Results show that mixing energy was lower as the IPS and MPT increase, which is intuitive since greater IPS and MPT values provide the particles with more space and improve their mobility (T. de Grazia et al., 2019).

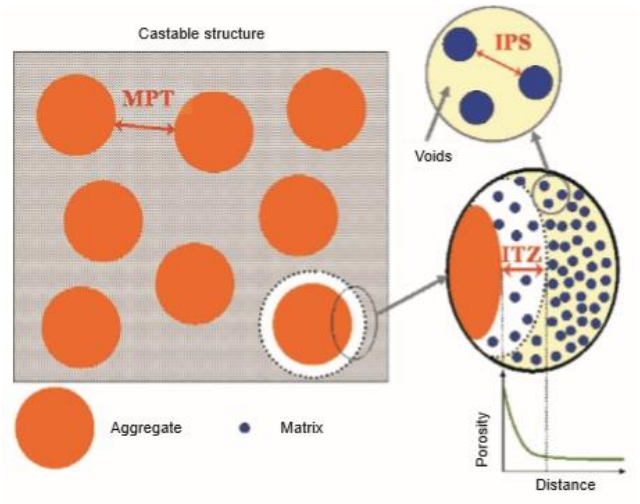

Figure 2.6 Representation of the IPS and MPT mobility parameters in a concrete mixture (Innocentini et al., 2003).

2.1.3 SUSTAINABLE CONSIDERATIONS

2.1.3.1 LIMESTONE FILLERS EFFECT

Besides the use of PPMS, PC reduction in concrete have been the focus of a number of studies in the past decade with increased attention to the use of limestone fillers as mineral admixtures and/or partial replacement of PC. Results in the literature show that limestone fillers are a promising alternative to PC reduction. Limestone fillers are by-products of the aggregate quarries industry which constitute an economic and sustainable alternative to partially replace PC in concrete (Knop & Peled, 2016). They exhibit ecological benefits when compared to PC due to the reduction of CO_2 emissions. Limestone fillers improve the rheological behaviour of cementitious materials (i.e. cement paste, mortar, and concrete made by PC) (Knop & Peled, 2016; Varhen et al., 2016). Moreover, they improve the microstructure of concrete and thus reduce its porosity and shrinkage (Varhen et al., 2016). Limestone fillers may enhance the hydration process at early ages by increasing nucleation sites for hydration products which raises the space available for hydration products precipitation (Berodier & Scrivener, 2014). Finally, limestone fillers may improve durability-related properties of the material, especially with regards to the ones linked to transport mechanisms (Vogt, 2010).

2.1.3.2 BINDER EFFICIENCY

Compressive strength of concrete at 28 days is the main parameter for structural design. PC hydration with water is responsible for generating calcium-silicate-hydrate (C-S-H) in the mix and thus mechanical properties. However, there is a misconception in the construction industry that increasing PC amount in the mixes raises the mechanical properties

(i.e. concrete strength) of the material. Considering the environmental impact of concrete, Damineli et al. (2010) proposed an index correlating the amount of binder required to produce one unit of concrete property (e.g. compressive strength). The author named it as the binder intensity index and it quantifies the eco-efficiency of concrete mixtures (Bruno L. Damineli, Kemeid, Aguiar, & John, 2010), which can be calculated through Equation 2.10.

$$bi = \frac{BC}{P} \qquad Equation\ 2.10$$

Where bi is the binder intensity index, BC is the amount of binder (kg/m^3), and P is the performance requirement (e.g. compressive strength - MPa). The index calculation does not require additional information and may facilitate the analysis of the environmental effects caused by different types of concrete. Moreover, to evaluate bi the authors selected 156 random Brazilian and international concrete mix-design records from distinct applications from 1988 to 2009 resulting in a total of 1585 data points as shown in Figure 2.7. Analyzing the plot below, it shows that for high strength concrete (i.e. > 50 MPa) mixtures are "naturally" more optimized since they incorporated lower bi factors than conventional concrete. On the other hand, conventional concrete (i.e. 20-40 MPa) shows to be often designed with moderate to high amounts of PC, demonstrating the need for techniques to improve their eco-efficiency. Moreover, data below illustrates that the majority of concrete produced worldwide presents PC contents ranging from 250 to 500 kg/m^3 and the vast majority of bi found in conventional concrete is close to or higher than 10 kg.m^3.MPa^{-1}.

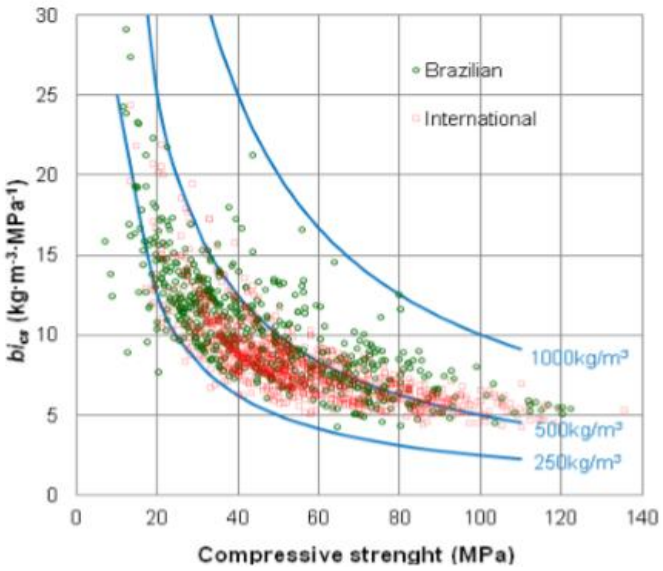

Figure 2.7 bi versus compressive strength from a) Brazilian data (green points); b) international data (red points) (Bruno L. Damineli et al., 2010).

2.2 FIBER REINFORCED CONCRETE

One of the drawbacks in concrete is its quasi-brittle behaviour, showing no ductility or deformation ability beyond the initiation of the first crack. Fibers are usually added in concrete to counteract its brittle behaviour, increasing ductility and toughness, controlling cracks propagation and delaying concrete failure (Bentur & Sidney, 2007).

The use of fibers in the construction industry can be tracked back down ancient history around different parts worldwide. Straws, or horsehairs were used in mud bricks in ancient Egypt, while early Chinese and Japanese housing markets used straw mats as reinforcement (around present day Baghdad); the first use of fibers in cementitious composites was introduced in 1874 (Bentur & Sidney, 2007; Raman, Jumaat, Bin Mahmud, & Zain, 2007).

In modern days, scientific development and research on the use of fibers in cementitious composites started to increase rapidly since the 1960s, where different types of fibers were developed with distinct cementitious composites formulations. For the purpose of simplification, fiber reinforced concrete is defined as a material that consists of a hydraulic cement such as PC, water, discrete fibers, and aggregates with different sizes. Currently, there are 200,000 metric tons of fibers being used as reinforcement in concrete; the main applications of fibers in the construction industry are in precast members, tunnel linings, airway pavements and sidewalks (Nemkumar Banthia, Bindiganavile, et al., 2014; Nemkumar Banthia, Zanotti, et al., 2014). Fibers sources are either natural (i.e. Cellulose, Sisal, and Jute)

or man-made fibers (i.e. glass, polypropylene, and steel fibers). Steel fibers are the most used type of fibers in concrete; they are more commonly used in dams, pavement, and shotcrete (Z. Li, 2011; Moghimi, 2014). Steel fibers present high elastic modulus and stiffness providing concrete with increased toughness, ductility, flexural and tensile strength, and increased impact, fatigue and absorption resistance (Grünewald, 2011; Moghimi, 2014; Raman et al., 2007). Steel fibers have a significantly higher specific gravity than concrete, which is considered a disadvantage by increasing the dead load of concrete.

The second most used type of fibers are polypropylene fibers; they fall under the category of synthetic fibers. Although polypropylene fibers present low tensile strength and modulus of elasticity, they are effective in enhancing the flexural strength, splitting tensile, toughness and durability performance of concrete. Polypropylene fibers are considered as chemically inert and non-corrosive materials (Guerini et al., 2018; Z. Li, 2011; Moghimi, 2014; Raman et al., 2007). However, their hydrophobic nature leads to poor adhesion bond with concrete since they present no water absorption ability. Advantages of Polypropylene includes low cost of raw materials, high alkali resistance, and high melting point (165^{o}c) (Bentur & Sidney, 2007). On the other hand, polypropylene fibers are sensitive to oxygen, sunlight, and are poor fire resistance (Moghimi, 2014).

In their early development days (i.e. 1950s-1960s), fibers were produced with a discrete short straight smooth sectional profile. Nowadays, they can be found with distinct sectional profiles (i.e. wavy profile, hooked end, and crimped ends) and textures to improve mechanical anchorage and bond with the cementitious matrix. Fibers are generally manufactured with varying lengths ranging from 10 to 70 mm. Along with the diameter, they present an important factor: aspect ratio (i.e. ratio of length to mean diameter), which significantly affects the main properties of concrete in both fresh and hardened state.

Plain cementitious composites are known to present a very low tensile strength, and negligible ductile behaviour, termed as brittle materials. Reinforcement rebars are added to concrete in certain and specified locations to resist the tensile and shear stresses that plain concrete can't withstand. On the other hand, fibers are added and distributed randomly in the concrete medium, therefore they are not as efficient as conventional reinforcement in resisting tensile or flexural stresses. Yet, their close proximity increases their ability for cracking control (Bentur & Sidney, 2007; Steven H. Kosmatka, Beatrix Kerkhoff, 2002). Furthermore, fibers act as bridges by transferring stresses across a cracked section, resisting crack propagation, and leading to enhanced concrete overall performance (Moghimi, 2014).

Typically, the amount of added fibers added to concrete ranges from 0-5% as a percentage of the material's volume. Values ranging from (0.25%-2%) are often used in sections requiring high deformation, impact, and blast resistance such as precast piles, pavement sections, and tunnel linings. In thin sheet components, where conventional reinforcement bars are difficult to be incorporated, fibers are used as primary reinforcement and their content could exceed 5% by volume. In addition, they may be included as secondary reinforcement to enhance ductile behaviour beyond first crack (i.e. crack initiation), by controlling crack propagation caused by temperature and shrinkage volume changes (Nemkumar Banthia, Bindiganavile, et al., 2014; Bentur & Sidney, 2007; Labib, 2018; Raman et al., 2007).

2.2.1 FRESH STATE OF FRC

Fibers are long slender particles that may significantly reduce the workability of concrete; their effect on workability is due to four reasons: a) first, they present large specific surface areas which increases the demand of cement paste thickness to enable homogenous flow. This is usually reflected by increasing the water and consequently the binder content to keep the same fresh state behaviour and microstructure. Furthermore, in concrete incorporating stiff steel fibers, the mechanical interaction with coarse aggregates dominates the materials flow, where the fibers push apart aggregates that matches their size causing hindrance to their movement. Conversely, bendable fibers (i.e. polypropylene) fill the space among the aggregates due to their flexibility; thus the mechanical interaction with aggregates is much less pronounced but they can still form a network with aggregates and other fibers (Grünewald, 2011). Finally, sectional (i.e. crimped ends, hooked ends, and wavy profile) and texture improvements for enhanced mechanical anchorage can also adversely affect the flow of fiber reinforced concrete (Grünewald, 2011).

In order to efficiently achieve the modified mechanical response of FRC, fibers must be homogeneously distributed along the mixture. ACI committee 544 (2008) recommends using fibers with sizes 2-4 times larger than aggregates, avoid including large portions of coarse aggregates (more than 55% of aggregate skeleton by absolute volume), and overmixing (ACI Committee 544, 2008). Furthermore, initial slump of plain concrete should be 50-75 mm higher than the desired final slump of the FRC (ACI 544, 1999; ACI Committee 544, 2008).

2.2.1.1 FRESH STATE TESTING METHODS FOR FRC

As it was stated earlier, the use of FRC has evolved significantly in the past decades and moved from experimental small-scale individual projects to routine factory and field applications with the use of tens of millions of cubic meters each year globally. This drives an essential need to reviewing existing fresh state testing methods for different

engineering applications. It has been found that fibers stiffen the mixture, add stability, and reduce flowability under static testing conditions, whereas under dynamic testing conditions (i.e. vibration), the effect of fibers decreases and thus FRC may behave similarly to plain concrete (Johnston, 1984). The slump test is a common convenient and inexpensive test procedure that measures the materials consistency (i.e. slump under its own weight). The latter is not a good indicator of workability when using concrete in vibrated applications. Fibers cause hindrance to the movement of particles, decreasing the slump value as its volume and aspect ratio increase (ACI Comittee 544, 2017; Wedding, Balaguru, & Ramakrishnan, 2010). Hence, comparing FRC slump values with plain concrete might become questionable. Flowability of FRC can be effectively evaluated by measuring the mixing energy required to produce FRC to the intended casting conditions. Once preliminary testing has been established on a specific FRC mixture, and the mixture presented satisfactory handling and casting behaviours at a given consistency, the slump test may be then used for quality control of FRC (ACI Comittee 544, 2017). The VeBe test, prescribed in EN-12350-3, is a standard British testing method that measures the behaviour of concrete subjected to external vibration. The test effectively assesses the ease of which vibrated concrete can be placed, remoulded, compacted into casting conditions, and the ease of entrapped air to be expelled (ACI Comittee 544, 2017; Johnston, 1984). The test is performed by placing the apparatus on top of a vibrating table; fresh concrete is then placed and compacted in a conical slump cone. The mold is afterwards removed, and a transparent plastic disk is placed on the top of concrete. The vibrating table is then started, and the time for concrete to be remoulded into the shape of the container is recorded as the VeBe time. It is well established that the VeBe test is an acceptable test for evaluating FRC workability, and distinguishing mix-design changes. A number of researchers have used both the slump and the VeBe test to compare different FRC with distinct design mixtures, and processing techniques.

In the evaluation of FRC fresh state behaviour, a well-known trend is found where the materials flowability decreases with the increase in fiber volume and aspect ratio. These parameters can be correlated together as the fiber factor, described in Equation 2.11:

$$Fiber\ Factor = VF\% * {}^{Lf}/_{df} \qquad \text{Equation 2.11}$$

Where VF%: Volume of fiber fraction by volume of concrete, Lf: Fiber length (mm), and df: fiber equivalent diameter (mm).

Leung et al (2003) studied the properties of fresh polypropylene FRC under the influence of pozzolans, in which the VF% of fibers and w/c was kept constant at 0.2% and 0.5, respectively, except for one control mix containing no fibers. The consistency (i.e. slump value) decreased by 40% when fibers were added to the mix. Conversely, 10% replacement of PC with fly ash increased the slump by 10% in comparison to the mix with PC only, while 10% replacement of PC with silica fume yielded the same slump value as the 100% PC mixes. The latter was related to the increased water demand caused by the ultra-fine fraction increase. Furthermore, when fibers were added to the mixture, Vebe time increased by 50% for mixes with 100% PC content, while when fly ash was used as replacement, the VeBe time decreased by 30% from 100% PC content mixes. Otherwise, the use of silica fume significantly increased the VeBe time up to 50%, which was related to the fineness and high pozzolanic effect of silica fume which in turn increased the cohesiveness of the mixtures, requiring more energy to compact the concrete (Leung & Balendran, 2003).

De Figueiredo et al. (2015), analyzed the workability of steel FRC through the slump and VeBe test. In their work, different initial slump values (i.e. 5 cm, 10 cm, 15 cm, and 20 cm) of conventional concrete mixtures were selected prior to the addition of fibers. Results showed that final slump of SFRC mixtures decreased as fiber content was raised in the mixtures up to a zero slump value. The rate of slump decrease was higher for mixtures with higher aspect ratio fibers. Furthermore, SFRC mixtures with higher initial slump values required higher fiber contents to reach zero slump. This result validates the ACI committee 544 (1998) comment on increasing the initial target slump of plain mixtures prior to fiber addition to facilitate FRC consistency and overall workability. However, SFRC mixtures with different initial slump values showed no significant variation in VeBe time results. Finally, SFRC mixtures with a higher maximum aggregate size displayed lower flowability results, which was more pronounced as fiber content increased (Figueiredo & Ceccato, 2015).

Guerini et al (2018) studied the effect of steel and polypropylene fibers incorporating different fiber contents, and aspect ratios on the fresh properties of concrete. Results indicated that the addition of fibers slightly increased the air content in the mixtures. Furthermore, it was noticed that the consistency (i.e. slump) decreased linearly as a function of the fiber content. The scattering of consistency (i.e. slump) results increased as fiber content increased, which was more pronounced for mixtures with lower water-to-cement ratio. Finally, results displayed that mixtures with

polypropylene fibers showed lower loss of workability as a function of fiber content when compared to mixtures with steel fibers (Guerini et al., 2018).

A wide number of models are used to describe the rheological behaviour of cementitious systems. The most common one is the so-called Bingham model, where a linear shear stress vs shear rate relationship is found. Concrete may present different rheological behaviours where viscosity changes as a function of the torque applied (ACI Comittee 544, 2017; Dadsetan et al., 2017). These systems are better described by the Herschel-Bulkley model given in Equation 2.12, which is the most common non-linear model relating the shear stress and yield stress of the material (Larrard, Ferraris, & Sedran, 1998).

$$\tau = \tau o + \mathrm{K}\gamma^{n} \qquad Equation\ 2.12$$

Where τ is the measured torque, τo is the yield stress, describing the minimum stress required to initiate flow, γ is the speed of rotation (rev/m), K and n are numerical parameters determined by the least square method.

Whenever a material follows a shear thinning behaviour (i.e. its viscosity decreases as a function of the shear stress), n is lower than 1. Conversely shear thickening materials (presenting increase in viscosity as a function of the torque) display n values greater than 1. Figure 2.8 illustrates typical shear flow curves for a Herschel-Bulkley material (Larrard et al., 1998).

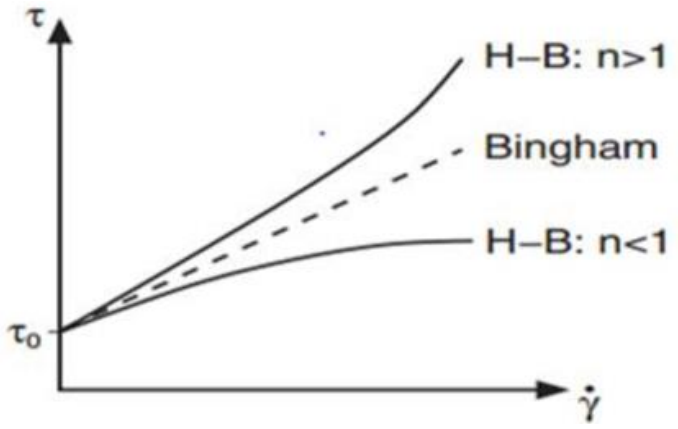

Figure 2.8 modelling of concrete as a Herschel-Bulkley fluid.

The addition of fibers to concrete often increases the yield stress of the material due to the interlock effect between fibers and aggregates at conditions which happens when the mix is at rest. Moreover during flow, mechanical contacts

between fibers and aggregates raises the viscosity of material. Laskar (2008) studied the effect of fiber content, and aspect ratio on the rheological properties of high performance FRC. Results indicate that shear stress slightly lessened as the fiber content increased from 0% to 0.25% Vf,, followed by a linear increase in shear stress as the fiber content raised from 0.25% to 2.0% Vf. Similarly, plastic viscosity decreased as the fiber content increased from 0 to 0.25%, followed by a linear increase in plastic viscosity as fiber content increased up to 2.0% Vf. The authors explained that the initial drop in yield stress and viscosity was due to an improved packing of the mixture at low fiber content. Furthermore, the yield stress raised as fiber aspect ratio increased from 25 to 125. However, the rate of increase in yield stress was more pronounced when the aspect ratio of the fiber increases from 50 to 125. Otherwise, the change in yield stress was insignificant when the aspect ratio increased from 25 to 50. Finally, plastic viscosity also raised as fiber aspect ratio increased; however, the change was insignificant (Laskar & Talukdar, 2008).

Pileggi et al. (2016) studied the effects of fiber content on the rheological properties of SCC. The results display a linear increasing relationship between fiber content and plastic viscosity. However, no significant impact on the shear torque is noticed when fiber content increase from 0% to 0.25% Vf. whereas from fiber content 0.5% and onwards, the shear torque increased proportionally with the increase of fiber content (Pileggi, R. G., Alferes Filho, R. S., Motezuki, Romano, & Figueiredo, 2016). Similarly, Banfill et al. (2006) studied the effect of carbon fibers on the rheological properties of fiber reinforced mortar. The results also showed an increase in both yield stress and plastic viscosity as the fiber content increased in the mixtures. Krage and Wallevik (2007) studied the effect of polymer synthetic fibers on the rheological properties of concrete. The increase in fiber content raised both yield stress and plastic viscosity (G. Krage, 2007). Finally, Grunewald (2004) studied the effect of fibers on the rheological behaviour of SCFRC and compared it to plain SCC. Results also displayed an increase in plastic viscosity and yield stress as the fiber content increased, which was more pronounced for mixtures with superior fiber aspect ratio (Grunewald, 2004).

2.2.1.2 THE EFFECT OF FIBERS ON PACKING DENSITY

One of the main challenges for accounting for fibers in PPMs proportioning is that PPMs consider that the shape of all particles within the system are spheres, while fibers in reality are rod shaped particles (Mangulkar & Jamkar, 2013). Therefore, the packing density of randomly distributed fibers might be lower than randomly distributed spherical particles. However, similar to spherical particles, the packing density of FRC rises when fibers are aligned in an orderly manner (Grünewald, 2011).

The compaction energy has a more important effect on the porosity of fiber packed systems than spherical particle systems. The porosity of fiber packed systems is higher when subjected to a low compaction energy and decreases significantly when the compaction energy is raised. Furthermore, stiff (i.e. steel) fibers push apart coarse aggregates, whereas flexible (i.e. polypropylene) fibers can be compressed by coarse aggregate particles and thus have a lower effect on the packing density of granular systems (Grünewald, 2011).

Milewski (1973) studied the packing effect of milled fibreglass and glass beads to characterize the packing of non-spherical particles combined with spherical particles. The results show that increasing the content of fibers in the system lessens the overall packing density, which was more pronounced for systems containing fibers with higher aspect ratios. Moreover, the packing density increased as the maximum spherical particle size decreased. Finally, the highest packing density was achieved when the length of the fibers was significantly higher than the maximum spherical particle size (Milewski, 1973). The latter aligns with the ACI committee 544 (1998) recommendation on using fibers with length 2-4 larger than the maximum particle diameter in FRC.

Yu et al (1993) proposed a method, the so-called "equivalent packing diameter", to account for fibers (i.e. non-spherical particles) into PPMs proportioning , given in Equation 2.13. In his approach, the authors proposed that the packing density is only related to the shape and dimensions of the particles within the system. Hence, the shape and dimensions of a non-spherical (i.e. fibers) particle can be related to the diameter of a fictitious sphere having an equivalent diameter; this approach should not, at least in theory, result in a change of the packing density of a mixture (A. -B Yu, Standish, & McLean, 1993).

$$dp = \left(3.1781 - 3.6821 * {}^{1}/_{\psi} + 1.5040 * {}^{1}/_{\psi^2}\right) * dv \qquad Equation\ 2.13$$

Where dp is the equivalent packing diameter, dv is the equivalent volume diameter, and is calculated through Equation 2.15 which calculates the diameter of a spherical particle with the same volume as the fiber, and ψ is the "sphericity" which is the ratio of the surface area of a sphere with the same volume of the fiber to the actual surface area of the fiber and is given in Equation 2.14 (A. -B Yu et al., 1993).

$$\psi = 2.621 * \left(\frac{{L/D}^{2/3}}{1 + 2(L/D)} \right) \qquad Equation\ 2.14$$

$$dv = 1.145 * \left(L/D\right)^{1/3} * D \qquad Equation\ 2.15$$

Where L and D are the length and diameter of the fiber, respectively.

Ferrara et al (2007) proposed the concept of (equivalent specific surface diameter) given by Equation 2.16 to include fibers in the mix-design of SCFRC using Alfred's model based on the assumption that the surface area of the total amount of fibers added to a unit volume of concrete has to correspond to the surface area of an equal mass of spheres having the same (average) specific weight of aggregates (Ferrara, Park, & Shah, 2007).

$$deq - fibers = \frac{3Lf}{1 + 2\frac{Lf}{df}} \frac{\gamma fiber}{\gamma aggregate} \qquad Equation\ 2.16$$

Where deq-fibers is the equivalent spherical particle diameter, Lf and df are the length and diameter of the fiber, respectively, γfiber is the specific weight of the fiber, and γaggregate is the weighted average specific weight of all the aggregates.

However, Yu et al (2012) applied the "equivalent packing diameter" and the "equivalent specific surface diameter" concepts to mix design SCFRC using Alfred's model. The results indicate that Equations 2.13 and Equation 2.16 do not follow experimental data gathered in the laboratory. In his approach the authors compared different SCC and SCFRC mixtures with straight steel fibers (Lf/df= 13mm/0.2mm). The equivalent packing diameter of a straight steel fiber (Lf/df= 13mm/0.2mm) is 5.6 mm based on Yu et al (1993) model, and 0.9 mm according to Ferrara's model whereas Yu et al (2012) found it to actually be 2.2 mm (Rui Yu, Spiesz, & Brouwers, 2012).

De Larrard (1998) studied the effect of fiber content and length on the packing density of distinct coarse and fine granular particle systems. The author proposed the concept of "perturbed volume" to include steel fibers into the mixtures designed through the compressive packing model (CPM)(de larrard, 1999). Results indicate that the packing density of coarse particles lowered as fiber content increased. Conversely, the fibers had little effect on the packing density of fine particles. Moreover, it was found that increasing the fiber length might raise the disturbance of aggregates located near the walls of the container, which in turn lessened the packing density of the system. Finally, it is worth noting that the "perturbed volume" concept does not apply to flexible fibers "i.e. glass, or polypropylene fibers) (de larrard, 1999).

Yu et al (2017) developed a sustainable ultra-high performance fibre reinforced concrete (UHPFRC) mixture proportioned through Alfred's model, where SCMS and fillers were used as PC replacement. In this work, fibers were added in the mixtures by volume without implementing them into the PPM. Results showed that the air content of the mix parabolically increased as the fiber content raised. Similarly, the porosity of the UHPFRC mixtures increased parabolically as the fiber content increased. Furthermore, the dilution effect of fillers led to an effective uniform dispersion of the fibers, which in turn enhanced the flexural performance of the UHPFRC. Finally, the use of PPMs to mix proportion UHPFRC resulted in a 30% reduction of PC with a reduced environmental impact by about 30% (Rui Yu et al., 2017).

Grunewald (2004) implemented Yu's (1993) and De Larrard' s (1998) models to include steel fibers in SCFRC mix-proportioned through the CPM. Results also indicated that the porosity of the granular system increased by the addition of fibers; the increase rate depended on the relative diameter of the aggregates particles to the fibers length (Grünewald, 2011). Finally, very few research (if any) is available on proportioning conventional vibrated FRC mixtures using PPMs, since most of the recent developments on mix-design procedures for fiber cementitious composites focus on UHPFRC and SCFRC.

2.2.2 MECHANICAL PROPERTIES OF FRC

Conventional concrete (plain concrete) requires reinforcement to be used as a construction material due to its low tensile strength, ductility and toughness. Historically, reinforcement has been adopted in the form of continuous rebars placed in the structural component at appropriate locations to withstand imposed tensile and shear stresses. On the other hand, fibers are randomly distributed throughout the matrix. Yet, their vicinity may make their behaviour better than conventional reinforcement for controlling crack propagation. Therefore, reinforcing concrete with fibers has been considered more efficient than conventional reinforcement (i.e. primary reinforcement) for certain applications such as thin sheet components where reinforcement bars cannot be used. In these applications, the fiber consumption can be relatively high and typically exceeds 5% by volume. Such a high amount of fibers increases both ductility and toughness of the composite. Fibers are also quite used in applications where components must locally withstand high loads or deformations, such as tunnel linings, blast resistant structures, or precast piles that must be hammered into the ground. Besides the above applications, fibers have been more often used as secondary reinforcement, mainly to provide post-cracking ductility to concrete components. The latter composites are referred to as conventional FRC

(Bentur & Sidney, 2007). Figure 2.9 illustrates the difference in the stress-strain relationship between (a) plain concrete matrix, (b) conventional FRC, and (c) high performance FRC.

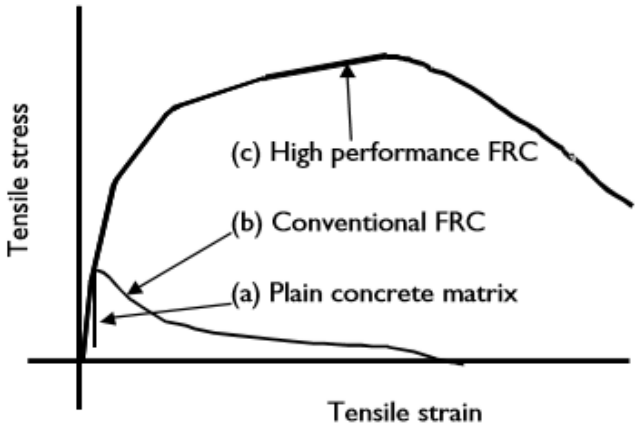

Figure 2.9 Typical stress-strain curves for plain concrete, conventional, and high performance FRC.

The addition of fibers may improve the durability performance of concrete due to crack propagation control (Granju & Balouch, 2005; Labib, 2018). However, compressive strength is barely affected in FRC(Grunewald, 2004; Z. Li, 2011; Raman et al., 2007). Furthermore, for an effective reinforcement performance, incorporated fibers must have a significantly higher modulus of elasticity, and a tensile strength 2-3 times higher than that of concrete (Naaman, 2003; Neville & Brooks, 2010). Also, the interfacial bond between fibers and matrix govern the stage where the composite failure and fiber pull out occurs at low bond strength (i.e. no crack propagation). Otherwise, the fiber rupture governs the behaviour at high bond strength (Abdallah, Fan, & Rees, 2018).

Abbas et al (2018) performed a comprehensive study on the effect of fiber content and length on the mechanical properties of FRC with different compressive strengths. In their work, compressive strength increased by 2% to 8% as fiber content increased from 0.5 to 1.5 Vf% for the higher strength concrete, while lower strength concrete exhibited 10% to 25% increase. The compressive strength increase was attributed to likely fibers confinement effects in concrete (Abbass, Khan, & Mourad, 2018). Unlike the compressive strength, the tensile strength showed a more pronounced improvement with values ranging from 11% to 47% for fiber content of 0.5% and 1.5%, respectively, when compared to plain concrete A linear relationship between increasing fiber content and tensile strength was then noticed (Abbass et al., 2018). Moreover, increasing fibers content from 0.5% to 1.5% resulted in increasing flexural strength from 3% to 124%, respectively, when compared to the plain concrete for fibers with lesser aspect ratio (i.e. 65). On the other

hand, at higher fiber aspect ratio (i.e. 80), flexural strength enhancement reached 140% compared to plain concrete. Furthermore, as the fibers length increased, the deflection at ultimate load of FRC increased regardless of fiber content; this behaviour was more noticeable for concretes with lower strength (Abbass et al., 2018).

Yazici et al (2007) studied the effect of aspect ratio (i.e. 45, 65, and 80) and fiber content (i.e. 0.5%, 1.0%, and 1.5%) on mechanical properties of SFRC. Results indicated 11-54% increase in split tensile strength of SFRC compared to plain concrete. Moreover, as the aspect ratio increased, split tensile strength increased at all fiber contents. The SFRC flexural strength exhibited a significant improvement ranging from 3% to 81% as compared to plain concrete; the results are more evident for high fibers content and aspect ratio (Yazici, Inan, & Tabak, 2007). Finally, Compressive strength of SFRC was 4% to 19% higher than plain concrete. Conforti et al. (2018) studied the effect of steel and macro-synthetic fibers (i.e. polypropylene) on concrete properties. Results show that the air content increased up to 15% with the addition of fibers, which was more pronounced for the polypropylene fibers. Furthermore, the compressive strength was not influenced by the addition of fibers, regardless of the fiber type. Finally, the flexural strength values were overall similar regardless of the fiber type. However, the mixture with steel fibers displayed a strain hardening behaviour at fiber content of 1.0 Vf% whereas the polypropylene fibers exhibited a strain softening behaviour characterized by a sharp drop after the peak load followed by a low post-peak residual strength (Guerini et al., 2018).

2.2.3 SUSTAINABLE FRC CONSIDERATIONS: AN OVERVIEW

Particle packing models (PPMs) have been used to optimize the particles skeleton of granular materials such as concrete to improve the fresh and hardened state performance of the material along with increasing its eco-efficiency. Previous studies demonstrate that the use of PPMs may reduce PC content in conventional mixtures from 20% to 50% (Fennis & Walraven, 2012; T. de Grazia et al., 2019). Yet, few research projects tried to use PPMs to optimize high-performance (or special features) FRC mixtures; some researches were conducted with the use of *Steel Self-Compacting Fibre Reinforced Concrete* (SSCFRC) (Cunha, 2014; Grunewald, 2004), *Engineered Cementitious Composites* (ECC) (V. C. Li, 2019), and *Ultra-high Performance Fiber Reinforced Concrete* (UHPFRC) (Rui Yu et al., 2017). Furthermore, very limited data is observed while the use of PPMs to enhance performance and sustainability of conventional FRC mixtures.

Normally, conventional FRC mixtures are design with tradicional techniques such as the absolute volume method (i.e. ACI method), which very often results in challenges in the fresh state along with moderate to high amounts of PC (i.e. PC contents > 450 kg/m^3) (ACI Comittee 544, 2014). Therefore, there is still a gap (and also an opportunity) in the literature to adopt advanced mix-design techniques such as PPMs to enhance the fresh state behaviour and eco-efficiency of conventional FRC systems while keeping suitable hardened state performance.

CHAPTER THREE: INVESTIGATION ON THE USE OF ALFRED MODEL TO MIX DESIGN ECO-EFFICIENT LOW CEMENT FIBER REINFORCED CONCRETE

3.1 ABSTRACT

Most of the fiber reinforced concrete (FRC) mixtures used in the construction market display important challenges in the fresh state. To solve this issue, very often moderate to high amounts of Portland cement (PC) and or admixtures are introduced which offsets the current efforts towards a more sustainable future of the construction industry. In this work, advanced mix design techniques (i.e. particle packing models – PPMs) are used to overcome the aforementioned issues and mix-proportion eco-efficient FRC with low cement content (< 300 kg/m3) and suitable behaviour in the fresh and hardened states. Twelve low cement (LC) FRC mixtures presenting a water-to-cement (w/c) ratio of 0.64 and containing different fiber types (i.e. polypropylene, and steel) with distinct contents (0.5% and 1.0% by volume) and lengths (38 mm and 50 mm) were proportioned. Two coefficients of distribution (i.e. 0.21, and 0.26) were selected for the PPM-designed mixes and evaluations on the fresh (i.e. VeBe time, slump and rheology) and hardened (i.e. compressive strength, and flexural behaviour) states were conducted. The performance of these mixtures are compared to control ACI proportioned mixes. Results showed that VeBe time raised with the increase of the fiber's length for high fiber content mixtures, whereas similar VeBe times were observed at low fiber content mixes. Similarly, increasing fiber content/length presented an increase in yield stress and plastic viscosity. Furthermore, PPM mixtures presented a shear thinning behaviour, while viscosity almost remained constant in the ACI mixtuures. Finally, results indicate that PPMs enable the development of eco-efficient low cement FRC mixtures with similar or improved performance in the hardened (i.e. compressive strength, and flexural performance) state with a lower environmental impact.

3.2 INTRODUCTION

Concrete is the most important construction material in the world due to its interesting mechanical and durability related properties, along with its relative low cost when compared to other building materials (e.g. steel), and the ability to be moulded into any given geometry in the fresh state. However, concrete presents a significant non-sustainable impact regarding carbon dioxide (CO_2) emissions, where it is responsible for up to 8 % of the yearly global CO_2 release (Andrew, 2017; Rui Yu et al., 2017). Portland cement (PC), concrete's most important ingredient, is the main responsible for its carbon footprint. The global PC production increased by 30-fold since 1950, and by 4-fold since 1990 (Andrew, 2017). Reducing PC content in concrete mixtures impacts directly on CO_2 emissions since the production of one ton of PC produces approximately one ton of CO_2 (T. de Grazia et al., 2019). In conventional concrete mixtures, the amount of PC required to bind the aggregate particles is relate to the packing density of the mix, which in turn depends on the particle size distribution (PSD) of the components selected. A number of mix-design approaches may be selected to proportion concrete mixtures, and among these, the ACI method (i.e. absolute volume method) is likely the most commonly used approach worldwide (Neville & Brooks, 2010). Although simple, the ACI method disregards important factors of the mix such as the PSD of the binder and aggregates, and thus is unable in many cases to proportion concrete mixtures with low embodied energy. Numerous advanced techniques were developed in the past decades to proportion concrete with low carbon footprint. Amongst those, particle packing models (PPMs) have stood out as a promising approach (Dadsetan et al., 2017; T. de Grazia et al., 2019).

3.3 BACKGROUND

PPMs are advanced mix-proportioning techniques whose main purpose is to decrease the intergranular voids of granular systems and thus increase packing density. The latter enables the development of concrete mixtures with low amount of binder and interesting behaviour in the fresh and hardened states (Mangulkar & Jamkar, 2013; T. de Grazia et al., 2019; R. Yu, Spiesz, & Brouwers, 2015). PPMs can be divided into two categories: discrete and continuous. Discrete PPMs aim for the maximum packing of "n" discrete size classes of particles, the so-called gap-graded systems (Yousuf et al., 2019). Otherwise, continuous PPMs intend to pack continuously sized particles available in the mixture with no gaps throughout the whole particle size distribution (PSD) (Mangulkar & Jamkar, 2013; Yousuf et al., 2019). The latter is considered compelling in concrete technology since most of the concrete components, at least in theory may be considered as presenting continuous PSDs. In 1907, Fuller and Thompson presented one of the first continuous

PPMs, the well-known "Fuller-Thompson" ideal grading curve according to Equation 3.1 (Fuller, W.B.; Thompson, 1907).

$$CPFT = (d/D)^n * 100 \qquad Equation\ 3.1$$

where CPFT is the cumulative percentage finer than d, d is the given particle size, D is the maximum particle size, and n was found to be optimal (i.e. maximizing packing density) from 0.45 to 0.5. Andreasen followed the works of Fuller and Thompson, and after some experimental testing and modelling, the author proposed an "ideal" curve known as the Andreasen model given in Equation 3.2, assuming that the smallest particle was infinitesimally small (Vogt, 2010).

$$CPFT = (\frac{d}{D})^q * 100 \qquad Equation\ 3.2$$

where CPFT is the cumulative percentage finer than d, d is the given particle size, D is the maximum particle size, and q is the distribution factor (q-factor). Andreasen suggested that the optimal q factor should range between 0.33 and 0.50, with minimum particle size d0 equal to zero (Andreasen, 1930). Funk and Dinger recognized that fine particles in real materials are finite in size and modified the initial Andreasen model considering the smallest particle size in the distribution. This approach gave rise to the so-called Alfred or modified Andreasen model as per Equation 3.3 (Funk & Dinger, 1994).

$$CPFT = \left(\frac{d^q - d_{min}^q}{D_{max}^q - d_{min}^q}\right) x\ 100 \qquad Equation\ 3.3$$

where CPFT is the cumulative percent finer than d, d is the given particle size, dmin is the minimum particle size, Dmax is the maximum particle size, and q is the distribution factor. The q factor may vary from 0.21 to 0.37, depending upon the workability requirement. The higher the q factor, the higher the amount of coarser particles in the system. After some testing and modelling, the authors claimed that the densest particle packing could be achieved with a q factor of 0.37, which would likely bring benefits to the short and long-term hardened state properties of concrete along with decreasing the binder content of the mixture. Otherwise, as the q factor increases beyond 0.37, the porosity of the system rises instantly, yet the same trend is not observed for q values lower than 0.37 (Yousuf et al., 2019).

Besides the use of PPMs, PC reduction in concrete may be achieved by using inert materials, the so-called inert fillers (Bruno L. Damineli, John, Lagerblad, & Pileggi, 2016; Rui Yu et al., 2017). These fillers are commonly used due to the physical benefits they bring to concrete, such as reducing porosity, the so-called "filler effect". Furthermore, it has been found that limestone fillers may present low reactivity with PC and thus change its hydration process due to the enhancement of nucleation sites (Varhen et al., 2016). The latter may result in an increase in the mechanical properties at early ages and improving the overall rheological behaviour of the material (Varhen et al., 2016).

Fibers are usually added in concrete to counteract its brittle behaviour, increasing ductility and toughness, controlling crack propagation and delaying concrete failure (Kuder, Ozyurt, Mu, & Shah, 2007; Naaman, 2003; Neville & Brooks, 2010). Currently, there are 200,000 metric tons of fibers being used as reinforcement in concrete (N Banthia, 2009). Fibers are effective for partially or totally replacing conventional reinforcement in non-structural and structural elements such as industrial floors, airway pavements, beams (shear reinforcement), precast members, and tunnel linings (N Banthia, 2009; Nemkumar Banthia, Bindiganavile, et al., 2014). Fibers of a wide range of materials and shapes are available; steel fibers being the most commonly used, although the use of polypropylene fibers have significantly improved in the past decade (Guerini et al., 2018). Fiber reinforced concrete (FRC) presents enhanced flexural capacities, impact and abrasion resistance, and greater toughness when compared to conventional concrete. Although FRC presents numerous advantages in the hardened state, the addition of fibers significantly worsens the fresh state behaviour of the material. Difficulties in mixing, transporting, handling and placing are conditions that may lead to poor compaction and thus compromise properties in the hardened state (Grünewald, 2011; Yazici et al., 2007). FRC mixes designed through conventional techniques often require high paste contents to overcome flowability issues, which results in a significant increase of PC amount and thus raises the carbon footprint of the material (Bentur & Sidney, 2007; Labib, 2018; Neville & Brooks, 2010; Rui Yu et al., 2017). Hence, optimizing FRC grading using PPMs along with inert fillers might be an appropriate approach to decrease the environmental impact of FRC while achieving a suitable fresh state behaviour. Finally, it is also important to quantify the efficiency of concrete mixtures based on performance and PC content. Damineli et al. (2010) have developed an index, the so-called binder intensity (bi) factor, which evaluates the eco-efficiency of a given concrete mixture by accounting for the PC or binder required to obtain 1 MPa of desired property such as compressive strength and can be calculated through Equation 3.4 (Bruno L. Damineli et al., 2010).

$$bi\ factor = \frac{BC}{f'c} \qquad Equation\ 3.4$$

Where bi factor is binder intensity factor (kg/m3.MPa-1), BC is the amount of binder content (kg/m3) and f'c is the compressive strength (MPa) at a specific age (i.e. 28-day). Bi factors commonly used in conventional concrete may vary from 9 to 14 kg/m3.MPa-1, regardless of its application (Bruno L. Damineli et al., 2010).

3.4 SCOPE OF THE WORK

As discussed in the previous sections, most of the FRC mixtures conventionally proportioned worldwide display either a non-sustainable character or some challenges in the fresh state. Therefore, this work aims to develop eco-friendly FRC mixtures designed through advanced techniques (i.e. continuous PPMs) with low cement content (<300 kg/m^3) and suitable performance in the fresh and hardened states. Twelve PPM mixtures were designed using the continuous Alfred model with distinct coefficients of distribution (i.e. q-factors: 0.21 and 0.26) and fiber parameters such as fiber type (steel and polypropylene), content (0.5%, and 1.0% V_f), and lengths (38 and 50 mm). All mixtures were assessed in the fresh (i.e. VeBe time, slump, and rheology) and hardened states (i.e. compressive and flexural strength). The performance of the PPM proportioned mixtures was then compared with six control ACI conventionally designed mixes with the same fiber parameters. Discussions on the suitability of using PPMs to proportion eco-efficient FRC concrete with interesting fresh and hardened properties is finally conducted.

3.5 MATERIALS AND METHODS

3.5.1 RAW MATERIALS CHARACTERIZATION

Table 3.1 and Figure 3.1 displays the characteristics of steel (S) and polypropylene (PP) fibers added in the mixtures. The fine aggregate (FA) selected for this research was a river sand and presents a PSD according to ASTM C33 (ASTM International, 2018) and a fineness modulus of 2.49. The coarse aggregate (CA) was a crushed limestone from Ottawa (Canada) with a nominal maximum size (NMS) of 19 mm. The PC selected was a GU type cement as per CSA A3001-18 (Canadian Standard Association, 2018) and its chemical composition obtained by X-ray fluorescence (XRF) analysis is presented in Table 3.2. A Limestone filler presenting similar PSD to cement was used to partially replace PC in the PPM mixtures. All PSDs of materials presenting particles smaller than 150 µm (i.e. PC and fillers) were determined through the use of laser diffraction, while larger particles were characterized through mechanical sieving, ensuring a representative sample as per ASTM C33 (ASTM International, 2018). The final size fractions of PPM designed mixes presented the following ranges: cement and fillers (≤ 150 µm), FA (150-300 µm, 300-600 µm,

600-1180 µm, 1180-2360 µm, and 2360-4750 µm), and CA (4750-9500 µm, 9500-12500 µm, and 12500-19000 µm). The size fractions of ACI proportioned mixes were kept the same in the coarse aggregate (CA) fraction, while it was not fully controlled in the fine fraction (i.e. only the fineness modulus of the sand was considered). Figure 3.2 displays the PSD of all raw materials used in this research.

Table 3.1 Characteristics of fibers (according to the manufacturer).

Type of fiber	Length (mm)	Diameter (mm)	Aspect Ratio	Volumetric diameter (mm)	Specific gravity (g/cm^3)	Fiber shape
Steel (S)	50	1.14	44	4.6	7.85	Wavy profile
Steel (S)	38	1.14	33	4.2	7.85	
Polypropylene (PP)	50	0.81	62	3.67	0.91	

Figure 3.1 Shape of fibers used in this project a) Steel fibers b) Polypropylene fibers

Table 3.2 Chemical composition of cement (according to the manufacturer).

Material	Compounds Content (%)									Blaine (m^2/kg)	Loss on Ignition (%)
	Na_2O	MgO	Al_2O_3	SiO_2	SO_3	K_2O	CaO	$CaCO_3$	$MgCO_3$		
Cement	0.14	2.66	4.92	19.53	3.86	0.77	61.91	-	-	381.46	2.24

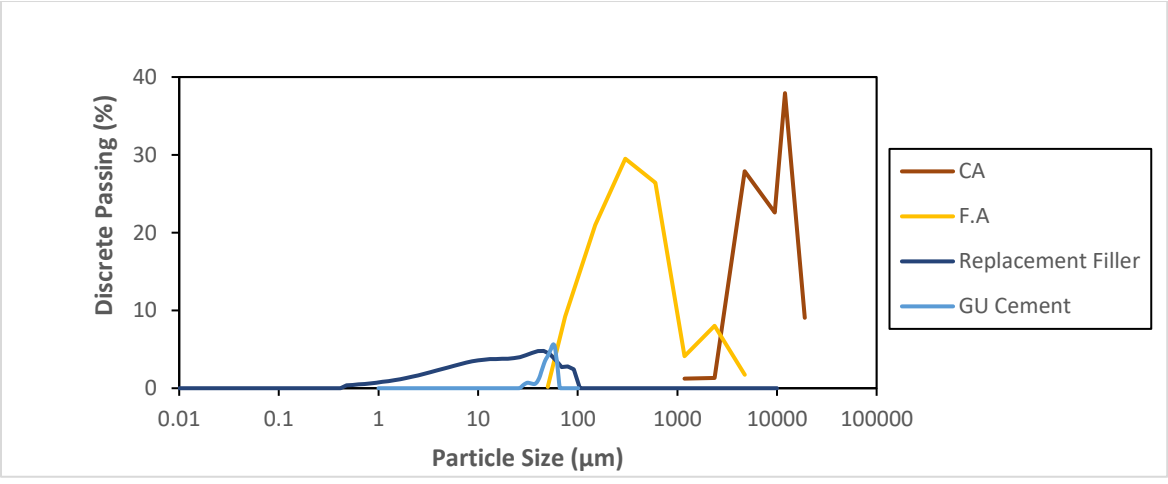

Figure 3.2 Particle size distribution of raw materials.

The specific gravity of PC and filler was determined by the pycnometer test using Helium gas (He). The specific gravity and the absorption of FA and CA for moisture correction was determined based on ASTM C128-15 and ASTM C127-15 (ASTM International, 2015c, 2015b), respectively. The results are summarized in Table 3.3.

Table 3.3 Raw materials characteristics.

Material	Specific Gravity (g/cm^3)	Absorption (%)
GU Cement	3.15	-
Replacement Filler	2.66	-
FA	2.73	0.79
CA	2.73	0.54

3.5.2 MIX DESIGN METHOD

Two main sets of mixtures were manufactured in this experimental program:

a) the first set consisted of twelve FRC mixtures designed through the PPM method, using two q-factors (0.21 and 0.26). The smallest and largest particle sizes were 2 µm and 19 mm. PC content was fixed at 300 kg/m^3 and the water-to-cement ratio was 0.64. A Limestone filler was used as a partial PC replacement by volume (due to their similar PSDs). S and PP fibers were added to the mixtures with 0.5% and 1.0% in volume (V_f). To incorporate the fibers in the PPM design, the equivalent volume diameter (dv) approach was used. This procedure aims to calculate the diameter of a fictitious sphere that has the same volume of the fiber (A. B. Yu & Standish, 1993). Thus, an equivalent dv was adopted to include fibers in the granular skeleton of the mixtures, according to Equation 3.5:

$$dv = 1.145 * \left({Lf}/{df}\right)^{1/3} . df \qquad Equation\ 3.5$$

where dv is the equivalent volume diameter (mm), L_f is the fiber length (mm), and d_f is the fiber diameter (mm). The fiber content (0.5% or 1.0% V_f) replaced the corresponding volumetric percentage of particles with an equal diameter (i.e. FA), which varied between 2360 µm and 4750 µm. A polycarboxilate based superplasticizer (SP) and a lignosulfonate based plasticizer (P) admixtures were used to enhance the flowability of the PPM mixtures without causing segregation. All PPM mixtures had the same admixtures content by PC mass. The dosages were fixed according to a maximum VeBe time of 25 s as per (Figueiredo & Ceccato, 2015; Johnston, 1984; Leung & Balendran, 2003).

b) the second set of mixtures consists of six control FRC mixtures designed by the ACI method (ACI Committee 211, 2004) following adjustments as per ACI 544.3r-08 (ACI Committee 544, 2008). The PC content was fixed at 375 kg/m^3 and the water-to-cement ratio was 0.64 (similar to PPM mixtures). An SP admixture was also used, as per the same concept applied for PPM mixtures and previously presented. Table 3.4 shows all the mix proportions. It is worth noting that the designation of the mixtures was based on the mix-design methods, type of fiber, fiber volume fraction, fiber length, and q-factor. For instance, a mixture named PPM-PP0.5-50-0.26 was designed through a PPM procedure with 0.5% PP, fiber length of 50mm, and q-factor of 0.26.

Table 3.4 Mix proportions of FRC.

Mixtures	Cement (kg/m^3)	Filler (kg/m^3)	FA (kg/m^3)	CA (kg/m^3)	Fibers (kg/m^3)	Water (kg/m^3)	Admixtures (SP + P)
PPM-S0.5-50-0.26	300	178	975	731	39	192	0.4% + 0.2%
PPM-S0.5-38-0.26					39		
PPM-PP0.5-50-0.26					4.5		
PPM-S0.5-50-0.21		277	961	645	39		
PPM-S0.5-38-0.21					39		
PPM-PP0.5-50-0.21					4.5		
PPM-S1.0-50-0.26		178	961	731	79		
PPM-S1.0-38-0.26					79		
PPM-PP1.0-50-0.26					9		
PPM-S1.0-50-0.21		277	947	645	79		
PPM-S1.0-38-0.21					79		
PPM-PP1.0-50-0.21					9		
ACI-S0.5-50	375	-	567	1115	38	240	0.2% + 0.0%
ACI-S0.5-38					38		
ACI-PP0.5-50					4.5		
ACI-S1.0-50			553		79		
ACI-S1.0-38					79		
ACI-PP1.0-50					9		

3.5.3 FABRICATION AND TESTING METHODS

Forty litres were produced for each mixture in an electric pan mixer, according to ASTM C192-16a (ASTM International, 2016). Fresh concrete samples were evaluated based on ASTM C172-17 (ASTM International, 2017). The slump test was performed as per ASTM C-143, and VeBe test were performed as per EN 12350-3 (ASTM C143, 2015; British Standards Institution, 2009) shown in Figure 3.3a. Rheological measurements were conducted through the IBB rotational rheometer, proposed by Tattersall (Tattersall, 1976) and modified afterwards (Beaupre, 1994) as shown in Figure 3.3b. The rheological profile was determined based on two-step process: (1) the speed of the impeller was increased in eight controlled stages up to a shear rate of approximately 43 rpm (acceleration process); and (2) the

rotation rate is decreased at the same stepwise until 2 rpm (each stage has at least two complete center shaft revolutions). The main rheological parameters (viscosity and yield stress) were determined as a function of the shear stress applied. It is worth noting that yield stress is the minimum torque enabling flow to the mixes, whereas viscosity (or apparent viscosity – AV) is considered in this work as the ratio between torque and rotation at the first deceleration point of the shear stress-shear rate curve.

Nine cylinders (Ø100 x 200 mm) were fabricated per mixture for compressive strength tests, according to ASTM C39 (ASTM International, 2015a). Two prismatic (150 x 150 x 400 mm) samples were cast for flexural analysis as per ASTM C1609 (ASTM C1609, 2012). All specimens were demoulded after 24 hours, ground and moist cured over time at controlled chamber with 23 ± 2 ºC of temperature. Compressive strength was gathered for all mixes at 7, 14, and 28 days of curing whereas the flexural analysis through the four point loading test shown in Figure 3.4 was only conducted at 28 days.

Figure 3.3 Fresh state testing setups a) VeBe Test setup b) IBB rheometer.

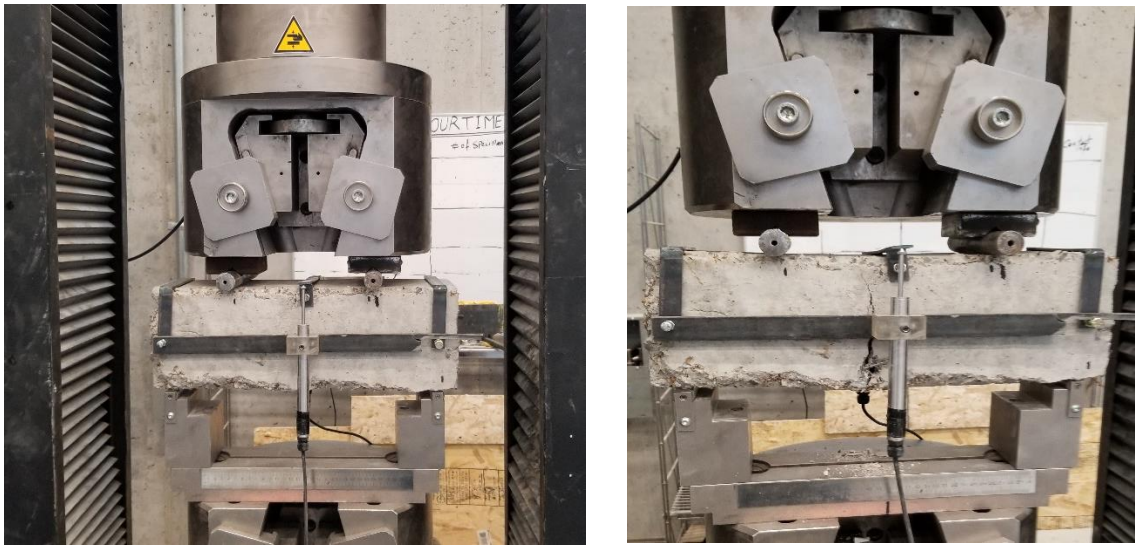

Figure 3.4 Flexural Strength test conducted on UTM of capacity 1000 kN by four-point loading at 28 days.

3.6 RESULTS PRESENTATION

3.6.1 FRESH STATE RESULTS

Table 3.5 present all results obtained for the slump test, VeBe test, and rheological characterization. The "applicable" and "non-applicable" terms indicate whether or not the rheology test could performed on each mixture, respectively, due to the torque capacity of the IBB rheometer.

Table 3.5 Fresh state results.

Mixtures code	VeBe test (s)	Slump test (cm)	Rheological Characterization
PPM-S0.5-50-0.26	7	10	**Applicable**
PPM-S0.5-38-0.26	6	4	**Applicable**
PPM-PP0.5-50-0.26	7	6	**Applicable**
PPM-S0.5-50-0.21	12	0	Non-applicable
PPM-S0.5-38-0.21	11	0	Non-applicable
PPM-PP0.5-50-0.21	10	3	Non-applicable
PPM-S1.0-50-0.26	18	2	Non-applicable
PPM-S1.0-38-0.26	11	5	Non-applicable
PPM-PP1.0-50-0.26	17	3	**Applicable**
PPM-S1.0-50-0.21	19	0	Non-applicable
PPM-S1.0-38-0.21	15	0	Non-applicable
PPM-PP1.0-50-0.21	24	0	Non-applicable
ACI-S0.5-50	3	14	**Applicable**
ACI-S0.5-38	2	15	**Applicable**
ACI-PP0.5-50	2	15	**Applicable**
ACI-S1.0-50	7	11	Non-applicable
ACI-S1.0-38	3	14	**Applicable**
ACI-P1.0-50	4	16	**Applicable**

3.6.2 VEBE AND SLUMP

Figure 3.5 shows the relationship between VeBe, slump, and fiber content for both PPM and ACI mixtures. Analyzing the results, one notices that in general, all ACI mixtures showed shorter VeBe times than PPM mixtures. Moreover, the higher the fiber content, the higher the VeBe time of all mixes. This impact was more pronounced on PPM mixtures. Furthermore, VeBe times for mixtures using S fibers were either similar or slightly longer than mixes with PP fibers for the same fiber length (50 mm). In addition, the higher the fiber length, the longer the VeBe time, for all mixtures. Finally, PPM mix-proportioned mixes with the distribution factor of 0.21 (i.e. higher amount of fines in the system) presented either similar or longer VeBe times than mixes with the distribution factor of 0.26.

The VeBe times recorded for ACI mixtures incorporating 50 mm fibers were 3 and 7 s for ACI-S0.5-50 and ACI-S1.0-50, respectively, whereas 2 and 4 s were measured for ACI-PP0.5-50 and ACI-PP1.0-50. ACI mixtures with shorter fiber length (38 mm) presented indeed the shortest VeBe time (i.e. 2 and 3 s for ACI-S0.5-38 and ACI-S1.0-38, respectively).

The VeBe times gathered for PPM mixtures with q-factor of 0.26 incorporating 50 mm fibers were 7 and 20 s for PPM-S0.5-50-0.26 and PPM-S1.0-50-0.26, respectively, while 7 and 17 s for PPM-PP0.5-50-0.26 and PPM-PP1.0-50-0.26; for PPM mixtures with a q-factor of 0.21 and 50 mm fibers yielded 12 and 20 s for PPM-S0.5-50-0.21 and PPM-S1.0-50-0.21, respectively whereas 11 and 24 s for PPM-PP0.5-50-0.21 and PPM-PP1.0-50-0.21. The VeBe times were shorter for 38 mm fiber lengths, especially for higher fiber contents. Values of 5 to 12 s were obtained for PPM-S0.5-38-0.26 and PPM-S1.0-50-0.26, respectively while 12 to 16 s were obtained for PPM-S0.5-38-0.21 and PPM-S1.0-38-0.21.

In terms of consistency (slump value), one verifies that as for VeBe times, all ACI mixtures showed lower consistency (i.e. higher slump values) than PPM mixtures. The higher the fiber content, the lower slump values of the mixes. This impact was slightly more pronounced for S fibers and PPM mixtures. Furthermore, the fiber length seemed to have negatively impacted on the slump, especially for PPM designed mixes. Finally, PPM mix-proportioned mixes with the distribution factor of 0.21 (i.e. higher amount of fines in the system) presented in general lower slump values than mixes with the distribution factor of 0.26. Slump values ranged from 18 to 10 cm for ACI mixtures, and 10 to 0 cm for PPM-mix-designed mixtures.

(a)

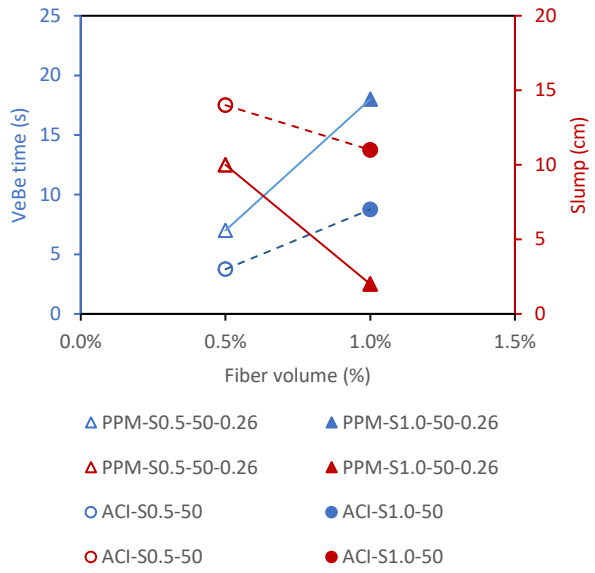

△ PPM-S0.5-50-0.26 ▲ PPM-S1.0-50-0.26

△ PPM-S0.5-50-0.26 ▲ PPM-S1.0-50-0.26

○ ACI-S0.5-50 ● ACI-S1.0-50

○ ACI-S0.5-50 ● ACI-S1.0-50

(b)

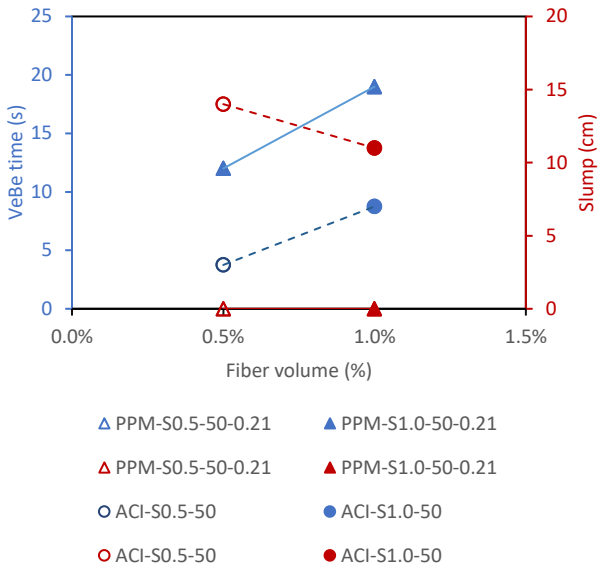

△ PPM-S0.5-50-0.21 ▲ PPM-S1.0-50-0.21

△ PPM-S0.5-50-0.21 ▲ PPM-S1.0-50-0.21

○ ACI-S0.5-50 ● ACI-S1.0-50

○ ACI-S0.5-50 ● ACI-S1.0-50

(c)

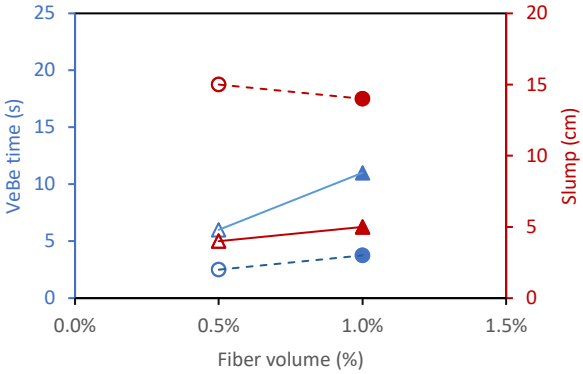

△ PPM-S0.5-38-0.26 ▲ PPM-S1.0-38-0.26

△ PPM-S0.5-38-0.26 ▲ PPM-S1.0-38-0.26

○ ACI-S0.5-38 ● ACI-S1.0-38

○ ACI-S0.5-38 ● ACI-S1.0-38

(d)

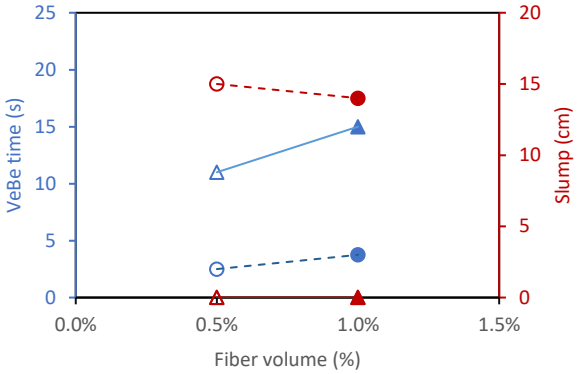

△ PPM-S0.5-38-0.21 ▲ PPM-S1.0-38-0.21

△ PPM-S0.5-38-0.21 ▲ PPM-S1.0-38-0.21

○ ACI-S0.5-38 ● ACI-S1.0-38

○ ACI-S0.5-38 ● ACI-S1.0-38

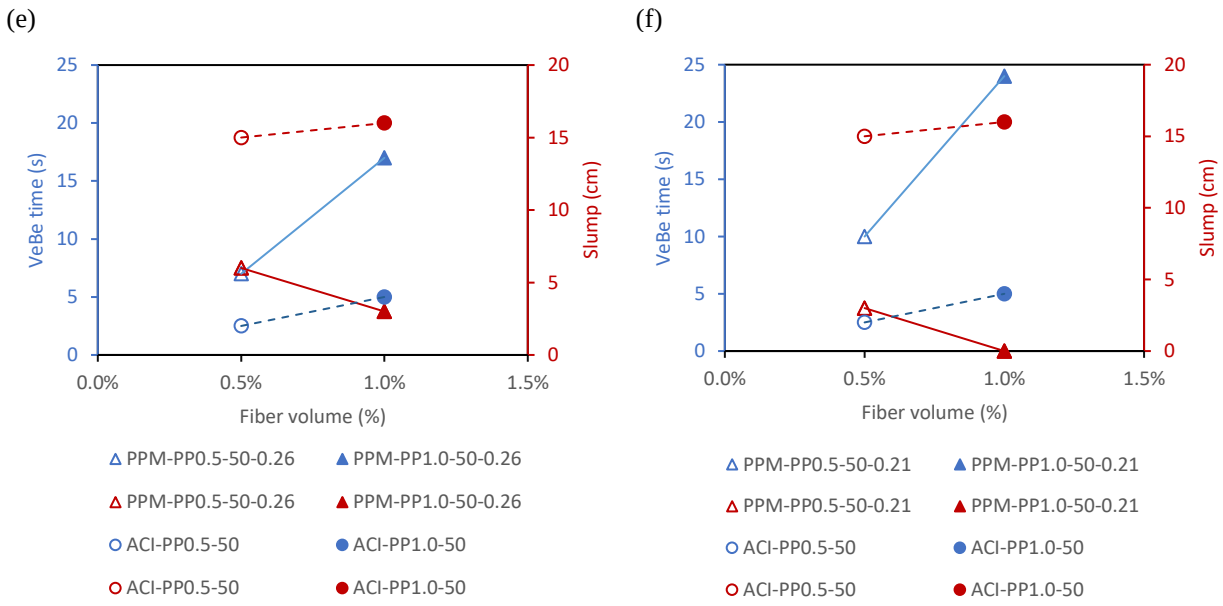

Figure 3.5 VeBe and slump tests of the distinct mixes as a function of fiber contents: (a) PPM (q-factor - 0.26) and ACI mixtures - fibers: S-50 mm; (b) PPM (q-factor - 0.21) and ACI mixtures - fibers: S-50 mm; (c) PPM (q-factor - 0.26) and ACI mixtures - fibers: S-38 mm; (d) PPM (q-factor - 0.21) and ACI mixtures - fibers: S-38 mm; (e) PPM (q-factor - 0.26) and ACI mixtures - fibers: PP-50 mm; (f) PPM (q-factor - 0.21) and ACI mixtures - fibers: PP-50 mm.

3.6.3 RHEOLOGICAL CHARACTERIZATION

Table 3.6 illustrates the rheological properties of ACI and PPM mixtures. It should be noted that the rheological properties of some mixes could not be measured due to the incapacity of the rheometer used (i.e. IBB) to appraise high consistency (or high viscosity) mixes at low torque regimes. Therefore, the rheological test did not apply for the following mixtures: ACI-S1.0-50; PPM-S1.0-50-0.26; PPM-S1.0-38-0.26; and all PPM mixtures with q-factor of 0.21.

Table 3.6 Rheological properties of analyzed mixtures

Mixture Name	Measured properties	
	Minimum Torque (N.m)	Apparent Viscosity (N.m/rpm)
PPM-S0.5-50-0.26	27.48	0.89
PPM-S0.5-38-0.26	23.50	0.84
PPM-0.5PP-50-0.26	7.00	0.52
PPM-1.0PP-50-0.26	15.61	0.51
ACI-S0.5-50	0.40	0.09
ACI-S0.5-38	0.26	0.03
ACI-S1.0-38	0.90	0.02
ACI-PP0.5-50	0.20	0.03
ACI-PP1.0-50	0.20	0.08

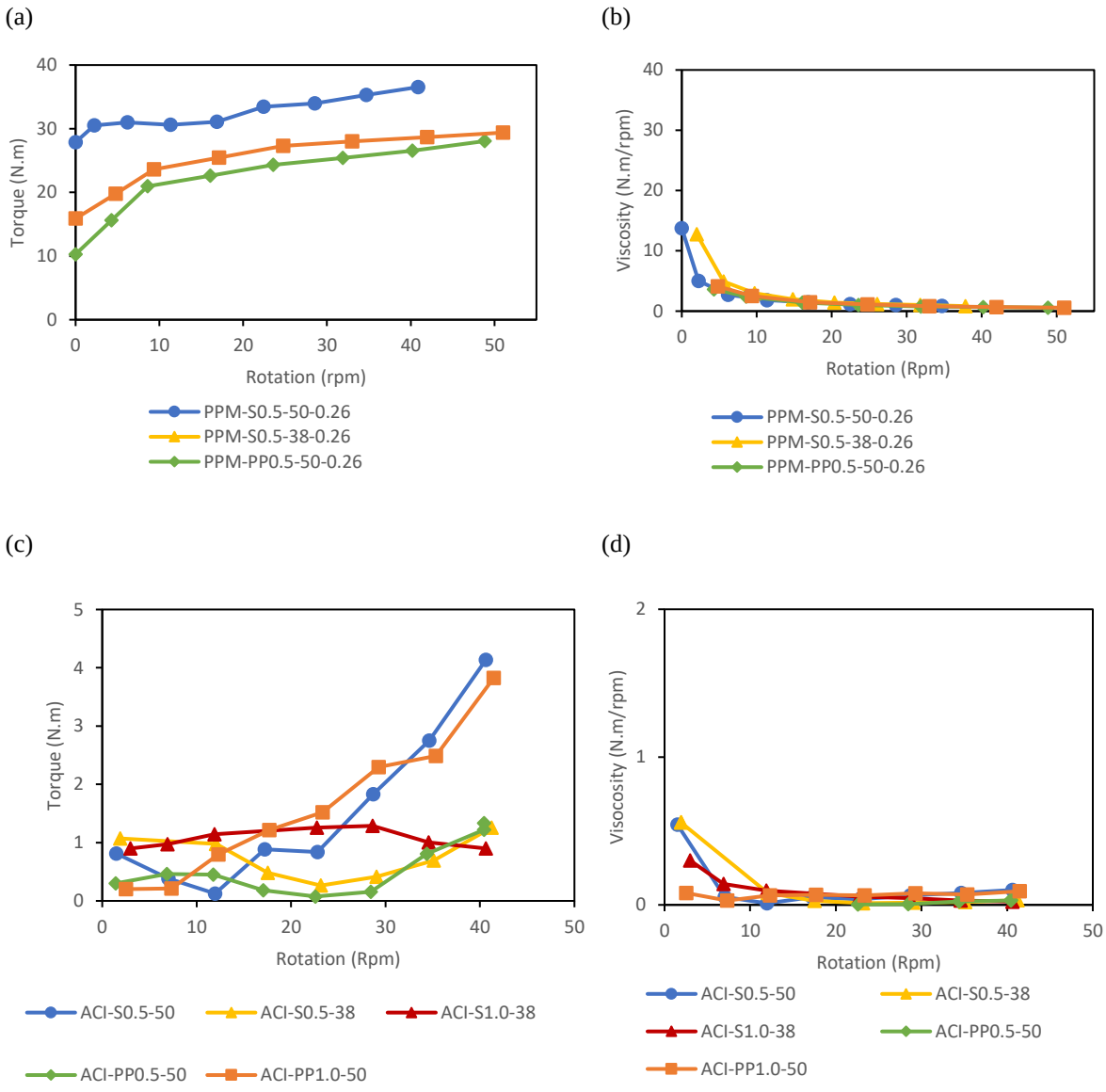

Figure 3.6 Rheological behaviour of the mixtures. Torque-rotation curves: (a) PPM mixtures and (c) ACI mixtures. Plastic viscosity-rotation curves: (b) PPM mixtures and (d) ACI mixtures.

Figure 3.6a and c displays the relationship between torque and rotation of PPM and ACI mixtures, respectively. Likewise, Figure 3.6b and d refers to the apparent viscosity (AV) as a function of rotation of PPM and ACI mixtures.

Analyzing the results, it can be noticed that in general, all ACI mixtures presented lower minimum torque (i.e. yield stress) when compared to PPM mixtures; the AV values gathered were not significantly different tough. Furthermore, the higher the fiber content, the higher the minimum torque required. This impact was more pronounced for PPM

mixtures. The minimum torque for mixtures incorporating S fibers was higher than mixes with PP fibers, regardless of fiber content, or length. The difference in minimum torque according to fiber type was more pronounced for PPM mixtures. Finally, the higher the fiber length, the higher the minimum torque, for all mixtures.

The minimum torque recorded for ACI mixtures containing 50 mm fibers was 0.40 N.m for ACI-S0.5-50, whereas 0.20 N.m was measured for both ACI-PP0.5-50 and ACI-PP1.0-50. ACI mixtures with shorter fiber lengths (38 mm) presented minimum torque values of 0.26 and 0.90 N.m. Likewise, the minimum torque gathered for PPM mixtures with q-factor of 0.26 incorporating 50 mm fibers were 27.48 N.m for PPM-S0.5-50-0.26, while 7 and 15.61 N.m for PPM-PP0.5-50-0.26 and PPM-PP1.0-50-0.26, respectively, presenting indeed the lowest minimum torque results. Finally, the minimum torque for shorter fiber lengths (38 mm) recorded was 23.50 N.m for PPM-S0.5-38-0.26.

In terms of AV (apparent viscosity), tt can be verified that all ACI mixtures showed lower AV than PPM mixtures However, the differences were not very important. Furthermore, the higher the fiber content, the higher the AV values for ACI mixtures with PP fibers., whereas the mixtures with S short fibers (38 mm) displayed similar AV as a function of fiber content. Conversely, PPM mixtures with PP fibers displayed similar AV values as fiber content increased.

AV values for PPM mixtures incorporating S fibers were higher than mixes with PP fibers, regardless of fiber content, or length. Otherwise, the ACI mixtures with long S fibers displayed the highest AV, followed by the PP fibers, and finally, the mixtures with S short fibers displayed the lowest AV. In addition, the fiber length negatively impacted on the AV for all mixtures, which was more pronounced for ACI mixtures. The AV recorded for ACI mixtures incorporating 50 mm fibers was 0.09 N.m/rpm for ACI-S0.5-50, whereas 0.03 and 0.08 for ACI-PP0.5-50 and ACI-PP1.0-50 respectively. ACI mixtures with shorter fiber length (38 mm) presented AV of 0.03 and 0.02 N.m/rpm for ACI-S0.5-38 and ACI-S1.0-38, respectively.

The AV values gathered for PPM mixtures with q-factor of 0.26 incorporating 50 mm fibers was 0.89 N.m/rpm for PPM-S0.5-50-0.26, while the lowest AV recorded was 0.52, and 0.50 for PPM-PP0.5-50-0.26 and PPM-PP1.0-50-0.26, respectively. Finally, the AV recorded for shorter S fibers (38 mm) was 0.84 N.m/rpm for PPM-S0.5-38-0.26. Finally, the viscosity of most ACI designed mixtures remained almost constant as a function of the torque applied. Otherwise, PPM mixtures exhibited a decrease in viscosity as a function of the torque applied (i.e. shear thinning behaviour), where a certain amount of energy (i.e. yield stress or minimum torque in this work) is required to induce flow.

3.6.4 HARDENED STATE RESULTS

- **COMPRESSIVE STRENGTH**

Figure 3.5a and c presents the evolution of the compressive strength over time. The results are the average of three specimens for all mixtures at 7, 14, and 28 days. Analyzing the results, it can be noticed that all PPM mixtures showed higher compressive strength than ACI mixtures. The improvement at 28 days ranged from 30% up to 70% depending on the type of fiber or fiber length. Thus, the compressive strength varied from 32.6 up to 36.4 MPa for PPM mixtures and from 20.3 up to 26.0 MPa for ACI mixtures. It is worth pointing that different mix design methods have the same water-to-cement ratio, which indicates the superiority of the results from PPM mixtures over ACI mixtures.

The increase of fiber content did not cause a significant improvement in the results of PPM and ACI mixtures since the maximum scattering obtained was 13%. Furthermore, ACI mixtures with long S fibers (50 mm) showed an improvement of 18% over short S fibers (38 mm) and PP fibers. Otherwise, the latter has not been verified for PPM mixtures since the difference was less than 5%, regardless the fiber type (S or PP fiber) or length (50 or 38 mm).

Figure 3.7a shows that PPM mixtures with long S fibers (50mm) presented the average increase of 36% over ACI mixtures at 28 days. However, it was not seen a significant difference in results between PPM mixtures with distinct q-factors (0.26 and 0.21). Likewise, the increment of fiber content (from 0.5% up to 1.0% V_f) did not impact the results since the variation was less than 7%.

Figure 3.7b evidences that PPM mixtures with shorter S fibers (38 mm) showed an average improvement of 53% over ACI mixtures at 28 days. Furthermore, the ACI mixtures revealed a growth of 15% in the compressive strength as fiber content raised from 0.5 to 1.0% V_f. Conversely, the variation in fiber content and q-factor did not cause a substantial difference among the results of PPM mixtures.

Figure 3.7c indicates that PPM mixtures with PP fibers exhibited an average rise of 57% over ACI mixtures. Furthermore, the increment of PP fiber content in ACI mixtures resulted in a slight improvement of 12% in compressive strength. As for the steel fiber mixtures, the change in fiber content and q-factor did not significantly influence on compressive strength results of PPM mixtures; the variation among the results was less than 4%. All the compressive strength results may be found in Table 3.7.

(a)

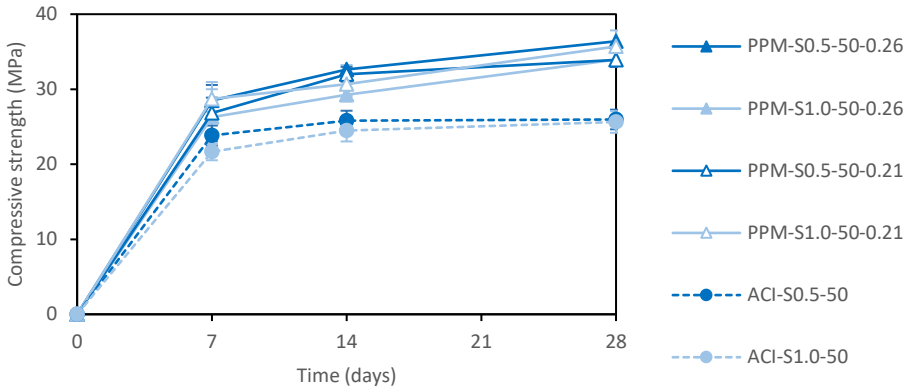

(b)

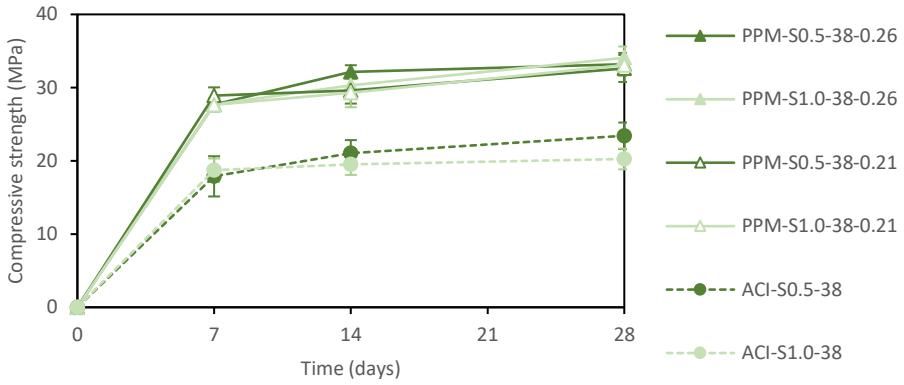

(c)

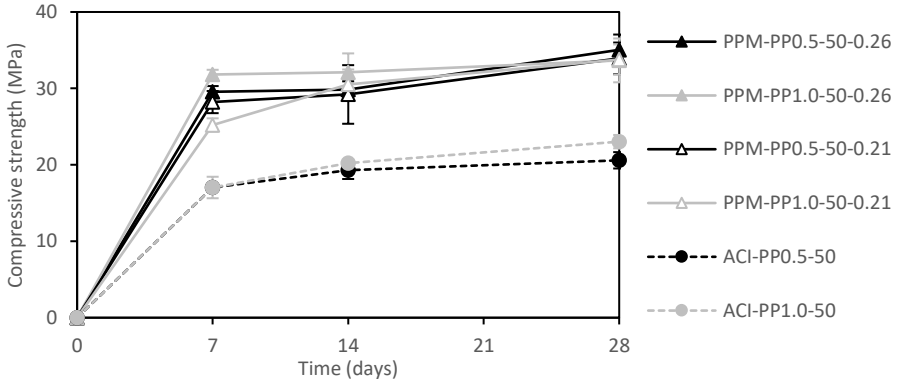

Figure 3.7 Compressive strength development as a function of time of concrete mixtures.

- **FLEXURAL ANALYSIS**

Table 3.7 displays the data obtained for all mixtures appraised in this research. Evaluating the data, one notices that the flexural strength (Modulus of Rupture - MOR) of PPM mixtures with 0.5% V_f of longer S fibers (50 mm) were

16% and 32% higher than the ACI mixture with a q-factor of 0.26 and 0.21, respectively. However, the MOR of PPM mixtures with 1.0% V_f of longer S fibers was 26% lower than the ACI mixture with a q-factor of 0.26, whereas for a q-factor of 0.21, there was no considerable difference between both mixtures. Furthermore, there was no relevant difference in the MOR of the mixtures with 0.5% V_f of shorter S fibers (i.e. 38 mm), since the variation between PPM and ACI mixtures was lower than 10% for both q-factors (0.26 and 0.21). However, with the increment of fiber content (1.0% V_f), the MOR of PPM mixtures containing shorter S fibers was 18% lower than the ACI mixture with a q-factor of 0.26, whereas the results were almost the same for q-factor of 0.21.

All PPM mixtures with PP fibers exhibited higher MOR values than ACI mixtures. PPM mixtures with a q-factor of 0.26 presented an increase of 33% and 36% higher than ACI mixtures with 0.5% and 1.0% PP fibers, respectively. Likewise, PPM mixtures with q-factor of 0.21 displayed a growth of 55% and 64% over the ACI mixtures with 0.5% and 1.0% PP fiber content, respectively.

Figure 3.8 illustrates the flexural load-stress-deflection curves of all ACI and PPM mixtures. The flexural stress values are calculated using Equation 3.6, as per ASTM C1609. Analyzing the plots below, one sees that all ACI mixtures showed an increase in the initial peak load (PL) and flexural stress at the first crack according to the increment of the fiber content from 0.5 up to 1.0% V_f as shown in Figure 3.8a. Moreover, among the ACI mixtures, the highest PL, and flexural stress was exhibited by 1% of longer S fibers. After the first crack, ACI mixtures presented an ascending load-deflection curve, followed by a descending load-deflection trend down to the specimen's failure. Almost all ACI mixtures with S fibers reached PL post- first crack; the only exception was seen for the 0.5% mix with short fiber length as shown Figure 3.6c. Conversely, ACI mixtures with PP fiber did not show the recovery of the load after crack up to PL, regardless of the fiber content as displayed in Figure 3.8e. Figure 3.8b refers to the flexural load-stress-deflection curves of the PPM mixtures with long S fibers (50 mm). It is noticed that the PL, and flexural stress increased in PPM designed mixtures when compared to ACI mixtures with a q-factor of 0.21, while it decreased for PPM mixtures with a q-factor of 0.26. However, it was very clear the improvement of the load at the post-cracking stage for PPM mixtures with high S fiber content when compared to the ACI mixtures

Figure 3.8d shows the flexural load-stress-deflection curves of the PPM mixtures with short S fibers (38 mm). Similarly, PPM mixtures with a q-factor of 0.21 displayed an increase in the PL when compared to ACI mixtures,

while it was not possible to see a clear trend from PPM mixtures with a q-factor of 0.26. Nevertheless, the improvement of PL increased with fiber content only for mixtures with a q-factor of 0.26.

Figure 3.8f presents the flexural load-stress-deflection curves of the PPM mixtures with PP fibers. Based on the results, all PPM mixtures with PP fibers displayed higher PL values than ACI mixtures, regardless of fiber content or q-factor. Furthermore, no improvement is noticed in PL as a function of fiber content increment. Nonetheless, PPM mixtures with a q-factor of 0.21 indicated higher PL than PPM mixtures with a q-factor of 0.26; this improvement corresponded to around 21%. After the first crack, almost all PPM mixtures with PP fibers did not regain the load at the same level of the PL; the only exception was showed by the mixture with 1.0% PP fiber and a q-factor of 0.26.

(a)

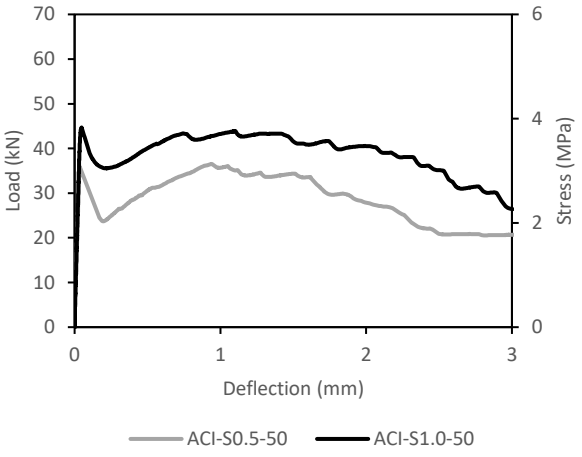

(b)

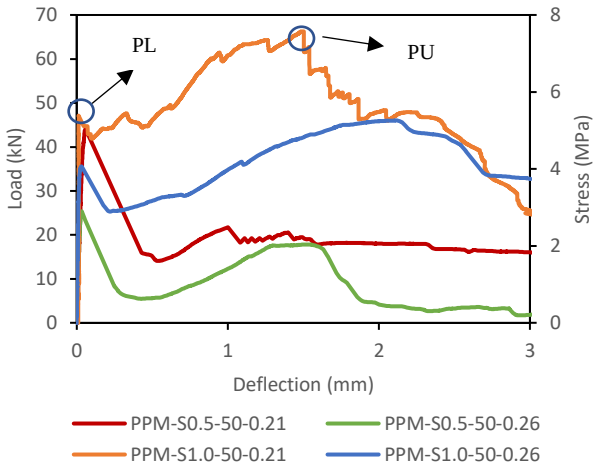

(c)

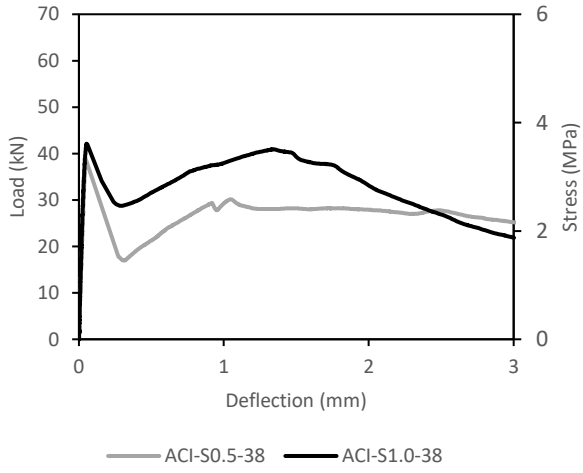

(d)

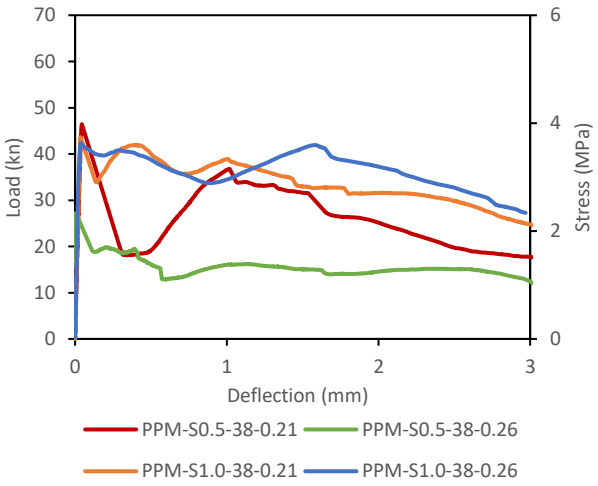

(e)

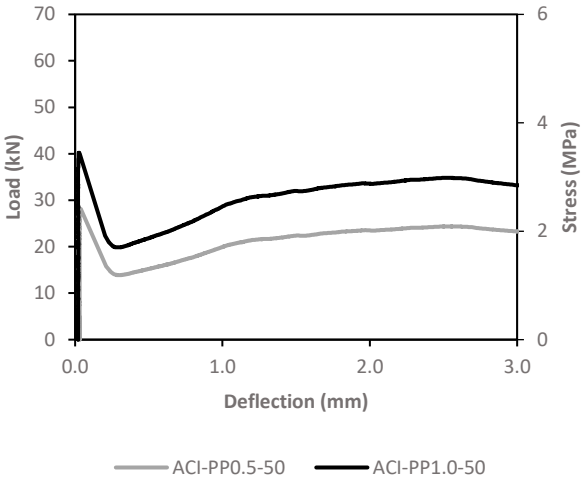

(f)

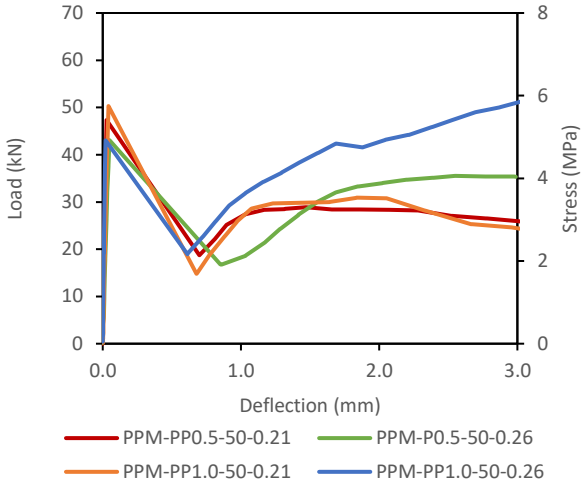

Figure 3.8 Flexural load-deflection curves of the ACI and PPM mixtures

Table 3.7 Hardened (i.e. compressive strength and flexural properties) state results of distinct mixes.

Mixture	Compressive strength (MPa)	CV (%)	Modulus of rupture - MOR (MPa)	Peak load (kN)	Toughness (J)
PPM-S0.5-50-0.26	36.4	4	4.3	24.1	63
PPM-S1.0-50-0.26	33.9	3	4.5	35.1	110
PPM-S0.5-50-0.21	33.9	3	4.9	42.5	80
PPM-S1.0-50-0.21	35.7	1	6.5	47.4	136
PPM-S0.5-38-0.26	33.2	5	4.2	24.2	42
PPM-S1.0-38-0.26	34.1	4	4.1	41.2	78
PPM-S0.5-38-0.21	32.6	6	4.3	44.1	80
PPM-S1.0-38-0.21	33.1	3	5.2	43.5	88
PPM-PP0.5-50-0.26	35.0	6	4.4	41.2	78
PPM-PP1.0-50-0.26	33.7	8	5.3	41.3	112
PPM-PP0.5-50-0.21	33.9	6	5.1	48.1	100
PPM-PP1.0-50-0.21	33.8	6	6.4	51.9	106
ACI-S0.5-50	26.0	5	3.7	32.2	102
ACI-S1.0-50	25.6	6	6.1	44.6	116
ACI-S0.5-38	23.4	8	4.7	39.1	85
ACI-S1.0-38	20.3	7	5.0	41.1	99
ACI-PP0.5-50	20.6	5	3.3	28.20	64
ACI-PP1.0-50	23.0	4	3.9	40.26	91

Figure 3.9a and b refers to the toughness results (area under the load-deflection curve up to 3 mm of deflection) for ACI and PPM designed mixtures, respectively. PPM mixtures with 0.5% of long S fibers presented lower toughness than ACI mixtures. The decrease obtained was 38% and 22% for q-factors of 0.26 and 0.21, respectively. However, PPM mixtures with 1.0% of long S fibers with a q-factor of 0.21 indicated the best behaviour throughout all mixes.

Invariably, PPM mixtures with short S fiber displayed a lower result than ACI mixtures, especially for a q-factor of 0.26. Otherwise, all PPM mixtures with PP fibers displayed higher toughness than ACI mixtures; PPM mixtures with PP fibers and a q-factor of 0.26 exhibited 22% higher toughness than ACI mixtures, regardless of fiber content. When a q-factor of 0.21 was selected, the rise in toughness was 15% higher when compared to ACI mixtures. All the toughness results (Joules) may also be found in Table 3.7.

(a)

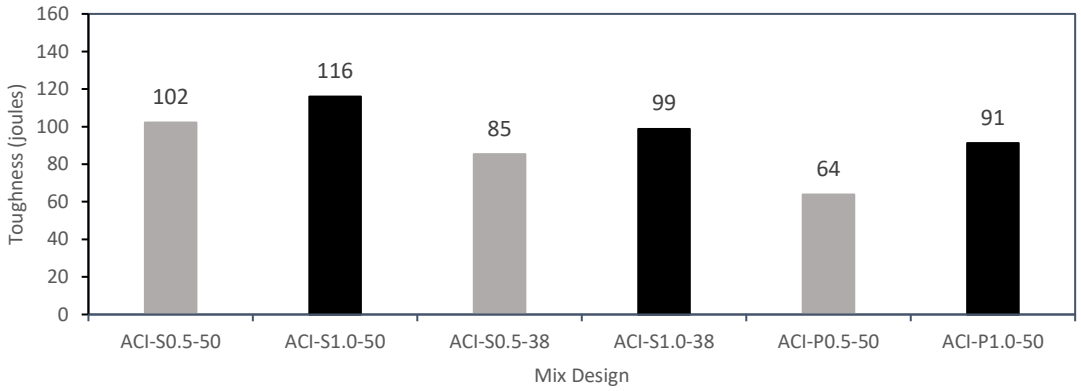

(b)

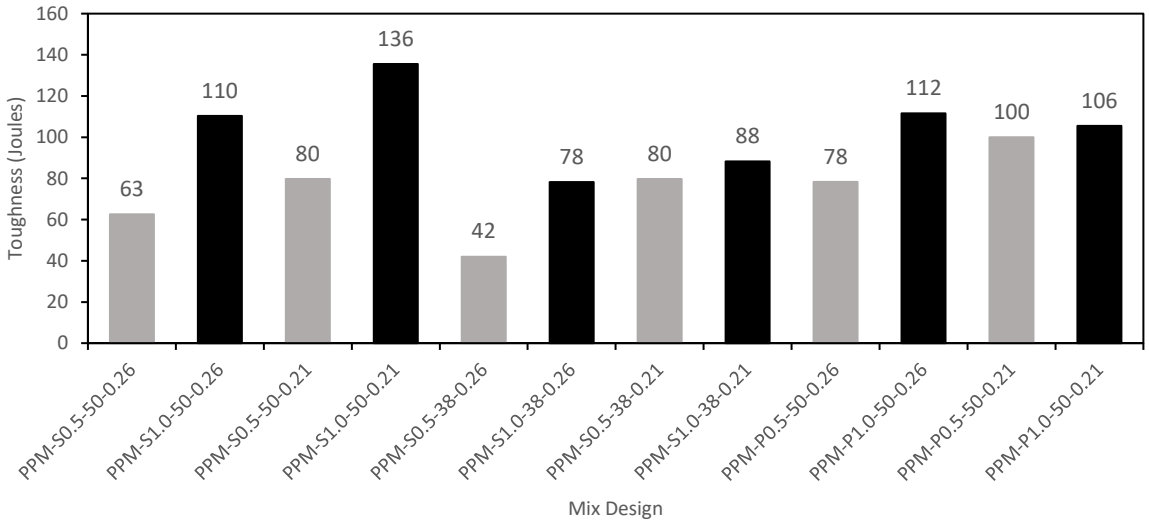

Figure 3.9 Toughness results of FRC mixtures a) ACI mixtures b) PPM mixtures.

Table 3.8 displays the residual load and stress values of the distinct mixes at a net deflection of L/600, and L/150. The residual stress was calculated following Equation 3.6, adopted from the American Standard Testing Method (ASTM) for flexural performance of FRC (ASTM C1609, 2012).

$$f = \frac{PL}{bd^2} \qquad Equation\ 3.6$$

Where:

f: strength (MPa), P: load (kN), L: span length in mm, b: the average width of the specimen at the fracture, and d: the average depth of the specimen at the fracture.

Results show that the residual stress and load values decrease as a function of the raise in deflection for most of mixtures with steel fibers, regardless of the mix-design method. Exception was only verified for the mixture PPM-S1.0-50-0.26 where the residual stress increased from 3.43 to 4.13 MPa as the deflection increased from L/600 to L/150. However, mixtures with polypropylene fibers displayed an increase in residual stress and load results at higher deflection values, regardless of the mix design method, or fiber content. Furthermore, the residual stress showed to increase as the fiber content increased for most of the PPM mixtures, except for mixtures containing polypropylene fibers designed with a q-factor of 0.21, where the residual stress decreased from 2.36 to 1.71 MPa, and 4.45 to 3.00 MPa at net deflections of L/600, and L/150, respectively. Similar to the PPM mixtures, the ACI mixtures displayed a raise in residual stress as the fiber content increased, except for the mixture with short steel fibers (i.e. 38 mm). Moreover, the residual load increased as the fiber content raised in PPM mixtures with steel fibers, except for mixtures with polypropylene fibers, and steel fibers designed with a q-factor of 0.26, where at net deflection of L/600 the residual load remained the same, or decreased. The ACI mixtures showed similar residual load behaviour to the PPM mixes, except for mixtures containing short steel fibers.

Table 3.8 Residual load and stress values of distinct mixes.

Mixture	P_{600}^{d} kN	F_{600}^{d} MPa	P_{150}^{d} kN	F_{150}^{d} MPa
PPM-S0.5-50-0.26	30.30	2.41	16.32	1.93
PPM-S1.0-50-0.26	29.00	3.43	34.88	4.13
PPM-S0.5-50-0.21	23.32	2.77	18.93	2.24
PPM-S1.0-50-0.21	48.26	5.72	33.50	3.97
PPM-S0.5-38-0.26	18.58	2.20	14.83	1.76
PPM-S1.0-38-0.26	24.60	2.92	22.94	2.72
PPM-S0.5-38-0.21	17.45	2.07	11.97	1.42
PPM-S1.0-38-0.21	32.20	3.81	23.56	2.79
PPM-PP0.5-50-0.26	16.58	1.97	32.26	3.82
PPM-PP1.0-50-0.26	17.66	2.10	41.31	4.90
PPM-PP0.5-50-0.21	19.92	2.36	37.50	4.45
PPM-PP1.0-50-0.21	14.45	1.71	25.28	3.00
ACI-S0.5-50	32.80	3.90	20.81	2.47
ACI-S1.0-50	51.80	6.13	32.82	3.90
ACI-S0.5-38	34.30	4.00	24.70	2.92
ACI-S1.0-38	31.95	3.80	22.63	2.70
ACI-PP0.5-50	17.50	2.10	0.00	0.00
ACI-PP1.0-50	24.00	2.84	34.53	4.10

P_{600}^{d}: residual load at net deflection of L/600 , F_{600}^{d} residual stress at net deflection of L/600.

P_{150}^{d}: residual load at net deflection of L/150 , F_{150}^{d} residual stress at net deflection of L/150.

3.7 DISCUSSION

3.7.1 QUANTIFICATION OF EFFICIENCY INDEXES IN CONCRETE

Mobility Parameters

Some works have reported the particle distance effects based on two mobility parameters: the Interparticle Separation Distance (IPS) and Maximum Paste Thickness (MPT). These parameters are often used in combination with PPMs to help explaining the behaviour of highly packed systems scuh as concrete in the fresh and hardened states.

IPS is the average distance separating fine particles in the cement paste and it represents the minimum amount of fluid (i.e. water) among particles (Grazia, 2018; Ortega et al., 2002). Thus, it is assumed that there is no particle agglomeration, and a part of the fluid in the paste fills the voids and covers the surface of particles, whereas the remaining fluid builds up the separating layer of particles (Ortega et al., 2002). IPS is described as per Equation 3.7:

$$IPS = \frac{2}{VSA}\left[\frac{1}{Vs} - \frac{1}{(1 - P_{of})}\right] \qquad Equation\ 3.7$$

Where IPS is the interparticle separation distance, VSA is the volumetric surface area of powder (m^2/cm^3), Vs is the volumetric solid fraction of powder, and P_{of} is the powder pore fraction at maximum packing condition. It is worth mentioning that powder is described in this work as materials with particle sizes smaller than 150 μm.

The Maximum Paste Thickness (MPT) provides the maximum separating distance of particles among the aggregates. It represents the amou of cement paste between two adjacent particles and is, described by Equation 3.8 (de Oliveira, Ivone R.; Studart et al., 2000; Grazia, 2018).

$$MPT = \frac{2}{VSA_c}\left[\frac{1}{V_{sc}} - \frac{1}{\left(1 - P_{ofc}\right)}\right] \qquad Equation\ 3.8$$

Where MPT is the Maximum Paste Thickness, VSA_c is the volumetric surface area of aggregate fraction (m^2/cm^3), V_{sc} is the volumetric solid fraction of aggregate fraction, and P_{ofc} is the aggregate pore fraction at maximum packing condition.

Efficiency factor of FRC

In order to account for the effect of fibers in FRC, a new parameter is proposed, the fiber-matrix factor (FMF), that is able to describe FRC properties based on the characteristics of the matrix and the fiber such fiber content and geometry, according to Equation 3.9:

$$FMF = \frac{IPS.MPT}{FF} \qquad Equation\ 3.9$$

Where FMF is the fiber-matrix factor (dimensionless), IPS is the Interparticle Separation Distance, MPT is the Maximum Paste Thickness, and FF is the Fiber Factor.

(Grünewald, 2011) has proposed the Fiber Factor parameter, which allows the correlation of the behaviour of the fresh and hardened state of FRC mixtures, as described in Equation 3.10:

$$FF = V_f.\left(\frac{L_f}{d_f}\right) \qquad Equation\ 3.10$$

Where FF is the Fiber Factor, V_f is the fiber content (%), L_f is the fiber length (mm), and d_f is the fiber diameter (mm).

Correlation among the efficient indexes and the properties of FRCs.

Table 3.8 displays efficient indexes values of the PPM mixtures and their corresponding VeBe time, toughness and compressive strength.

Table 3.8 Efficient index of the PPM mixtures.

PPM mixtures	Efficient Indexes			Properties of FRC		
	IPS	MPT	FMF	VeBe Time (s)	Toughness (J)	Compressive strength (MPa)
PPM-S0.5-50-0.26	0.59	1.00	0.03	7	63	36.4
PPM-S1.0-50-0.26	0.59	1.01	0.01	18	110	33.9
PPM-S0.5-50-0.21	0.45	1.03	0.02	12	80	33.9
PPM-S1.0-50-0.21	0.45	1.04	0.01	19	136	35.7
PPM-S0.5-38-0.26	0.59	1.00	0.04	6	42	33.2
PPM-S1.0-38-0.26	0.59	1.01	0.02	11	78	34.1
PPM-S0.5-38-0.21	0.45	1.03	0.03	11	80	32.6
PPM-S1.0-38-0.21	0.45	1.04	0.01	15	88	33.1
PPM-PP0.5-50-0.26	0.59	1.00	0.02	7	78	35.0
PPM-PP1.0-50-0.26	0.59	1.01	0.01	17	112	33.7
PPM-PP0.5-50-0.21	0.45	1.03	0.01	10	100	33.9
PPM-PP1.0-50-0.21	0.45	1.04	0.01	24	106	33.8

Figure 3.10 a and b displays the relationship between the mobility parameters (i.e. IPS, and MPT) and VeBe time for the distinct q-factors among the PPM mixtures. It is worth noting that no distinction of the mixtures according to fiber type,content,or length was given to effectively compare the q-factors and their relative mobility parameters. As shown in Figure 3.10a, each mixture with the same q-factor presented the same IPS value, however, a slight trend between the VeBe time and IPS is observed, where the IPS increases as the q-factor increases from 0.21 to 0.26, which in turn increased the flowability (decreased VeBe time). The latter is intuitive, since greater IPSs provide more space and improve mobility amongst the particles. Figure 3.10b displays the relationship between the MPT and VeBe time. Generally, it can be noticed that as MPT increases, VeBe time also increases. Similar to the IPS, greater MPTs provide more space and decrease the friction among aggregates. However, no clear relationship between the q-factor and the MPT is noticed, regardless of the fiber and matrix characteristics.

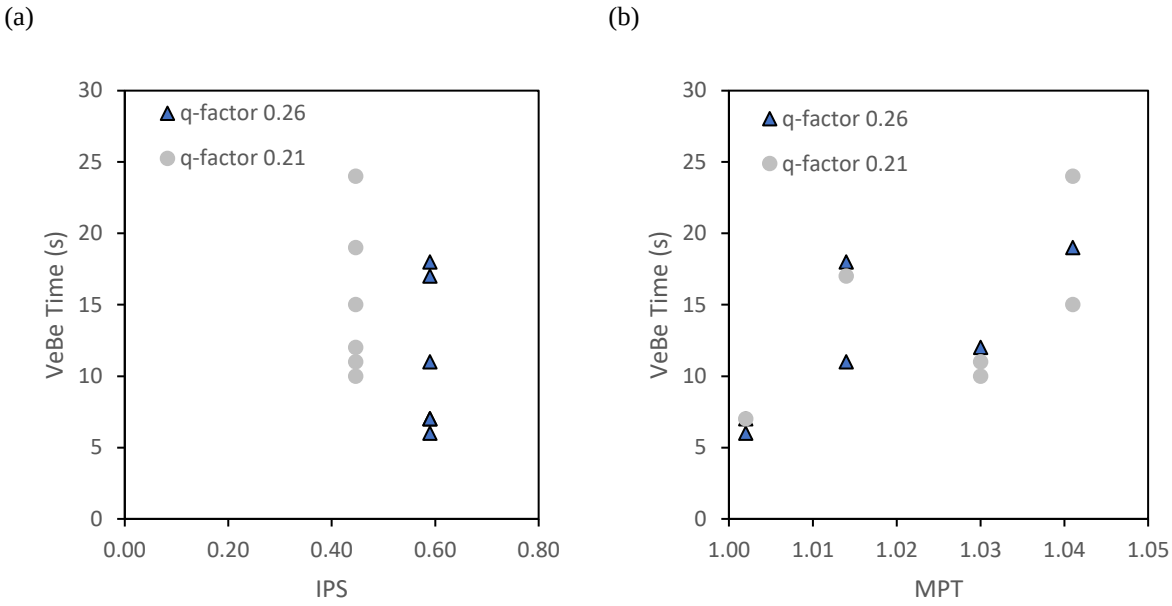

Figure 3.10 Relationship between (a) IPS and VeBe time (s); and (b) MPT and VeBe time (s).

VeBe time and toughness were selected to be correlated with FMF since these properties are extremely affected by the fibers. All PPM mixtures displayed a drop in VeBe time with the rise of FMF Figure 3.11a. The same trend was observed for toughness, which in turn decreased with the increase of FMF Figure 3.11b. This behaviour can be attributed to the reduction of the packaging capacity with the increase of FMF, which affects negatively the toughness and increases the flowability of the system. Therefore, the proposed FMF seems to be quite promising to describe the behaviour in the fresh and hardened states of FRC designed through PPMs with different PSD and fiber characteristics.

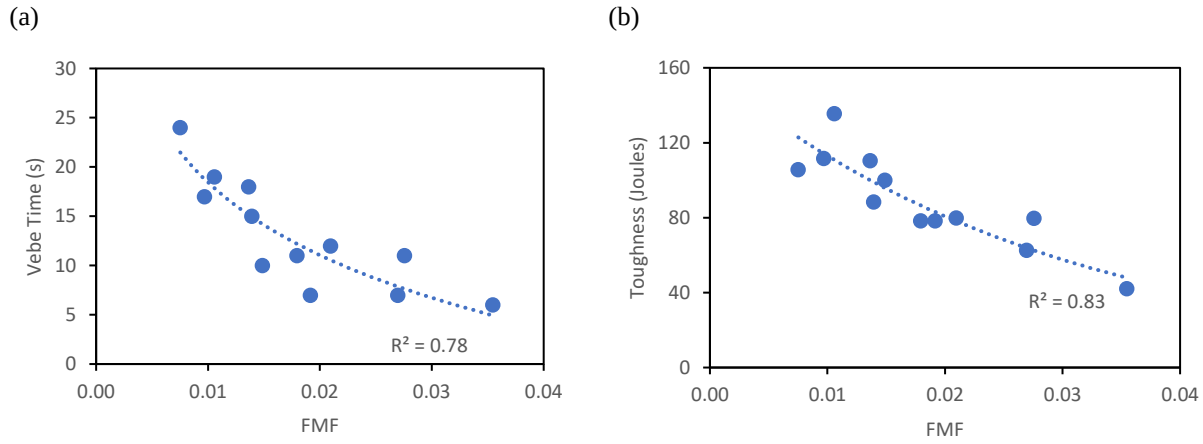

Figure 3.11 Relationship between FMF and (a) VeBe time (s); and (b) Toughness (j).

3.7.2 FRESH STATE PERFORMANCE

The addition of fibers very often negatively impacts the behaviour of concrete mixtures in the fresh state, due to the increase of friction (interlock effects) between the fibers and the coarse aggregate particles, which in turn raises the consistency and lessens the flowability of the mix at rest or low torque regimes. Yet, in practice, conventional FRC is always compacted through vibration (disregarding self-levelling systems), and under such a condition, FRC may yield completely different flowability behaviour. Thus, it is very important to perform tests that are able to "capture" the ease of consolidation of FRC mixtures under vibration and in this context, the VeBe test is considered an interesting procedure.

Based on the analyzed results, one may notice that PPM designed mixtures displayed higher VeBe times for increased fiber contents. The latter was even more pronounced for longer fibers, since likely the interlock effect with the coarse aggregate particles was greater. These results were quite expected, since ACI mixtures presented a much higher amount of binder (i.e. PC), which acted as a system "lubricant" and thus facilitated flow under torque. Moreover, PPM mix-proportioned mixtures presented lower initial porosity than ACI mixtures (which is inversely proportional to the amount of PC); this makes the distance between the particles (i.e. powders, aggregates and fibers) lower for these mixtures and may jeopardize flow. This trend was verified for both S and PP fibers; although one might have expected this trend to be higher for the S fiber when compared to PP due to its higher density, the PP fibers used in this work displayed a greater aspect ratio which might have offset the expected behaviour.

If only PPM proportioned mixtures are evaluated (q factors of 0.26 and 0.21), one notices two very interesting and contrasting behaviours, as follows: a) mixtures proportioned with steel fibers and a q-factor of 0.21 displayed a lower increase in VeBe time as a function of the fiber content; this mix is characterized by a higher amount of fines in the system (i.e. fillers), while the other presents a higher fraction of coarse aggregates. This result seems to indicate that the use of PPMs with lower q factors may be beneficial to proportion SFRC, decreasing the amount of coarse aggregates in the system and lessening the friction between fibres and coarse aggregates) and, b) mixtures proportioned with polypropylene fibers designed with a q-factor of 0.26 displayed a lower drop in flowability (VeBe time increase) as a function of the fiber content when compared to its companion mixtures designed with a q-factor of 0.21. Polypropylene fibers are flexible and can fill in the spaces between coarser aggregates, yet their flexibility mainly affects the flowability of the paste. This is very different from steel (and stiff fibers) that interacts mainly with the

coarse aggregate fractions. This phenomenon has been previously observed by (Figueiredo & Ceccato, 2015; Grünewald, 2011). Finally, all PPM mixtures designed with a q-factor of 0.21 showed longer VeBe times than their companion 0.26 q-factor mixes, regardless of fiber type, content, or length. This is very likely due to the higher amount of fines in the system which reduces the distance amongst the fine particles and thus increases the minimum torque to enable flow of the mixture.

The VeBe results obtained in this work were very comparable to the minimum torque data gathered while the use of the IBB rheometer; i.e. PPM mix-designed concrete presented higher minimum torque (or yield stress) and thus required a higher amount of torque to enable flow. The latter is exactly what has been indirectly measured by the VeBe test and discussed above. However, not that important differences of AV results were found for all mixtures (i.e. ACI and PPM mix proportioned), although their PC contents were quite different. PPM mix-proportioned FRC mixtures yielded a shear thinning behaviour and thus a decrease in viscosity was found as a function of torque. The latter means that PPMs may be a suitable technique to proportion FRC vibrated and/or pumped concrete, since low viscosity at high torque regimes is expected for materials applied in the field under these conditions.

3.7.3 FRESH STATE MODELLING

A wide number of models are used to describe the rheological behaviour of cementitious systems. The most common one is the so-called Bingham model, where a linear shear stress vs shear rate relationship is found. However, concrete mixtures may present different rheological behaviours where viscosity changes as a function of the torque applied (ACI Comittee 544, 2017; Dadsetan et al., 2017). These systems are better described by the Herschel-Bulkley model given in Equation 3.12, which is the most common non-linear model, and relates shear stress and yield stress (Larrard et al., 1998).

$$\tau = \tau o + \mathrm{K}\gamma^{n} \qquad Equation\ 3.12$$

Where τ is the measured torque (Pa.s), τo is the yield stress (Pa), describing the minimum yield stress required to initiate flow, γ is the speed of rotation (rev/m), K is the viscosity constant parameter and n is the flow behaviour factor; the latter are numerical parameters determined by the least square method.

Using the HB model, it is known that the material follows a shear thinning behaviour (decrease in viscosity as a function of the torque) when n < 1, a shear thickening behaviour (increase in viscosity as a function of torque) for n > 1, and for n=1 the material follows a Bingham rheological behaviour (T. de Grazia et al., 2019).

Table 3.9 Herschel-Bulkley model estimated parameters for the distinct mixtures.

Mixture Name	Herschel-Bulkley				Relative Error (%)	
	Yield Stress (N.m)	K	n	Plastic Viscosity (N.m/rpm)	Yield Stress (N.m)	Plastic Viscosity (N.m/rpm)
PPM-S0.5-50-0.26	28.82	0.25	0.91	0.88	5	1
PPM-S0.5-38-0.26	23.40	1.87	0.42	0.84	0	0
PPM-0.5PP-50-0.26	10.11	4.20	0.38	0.51	44	2
PPM-1.0PP-50-0.26	15.66	3.17	0.38	0.51	0	0
ACI-S0.5-50	0.00	0.01	1.49	0.08	100	7
ACI-S0.5-38	0.00	0.78	0.00	0.02	100	33
ACI-S1.0-38	0.19	0.74	0.06	0.03	79	23
ACI-PP0.5-50	0.00	0.10	0.57	0.02	100	33
ACI-PP1.0-50	0.00	0.09	0.95	0.08	100	3

Table 3.9 displays the estimated Herschel-Bulkley rheological parameters and the relative error of the yield stress and plastic viscosity, calculated through Equations 3.13 and 3.14 respectively, from the experimental results (i.e. minimum torque, and apparent viscosity) for all mixtures.

$$Yield\ stress\ relative\ error(\%) = \frac{minimum\ torque - yield\ stress}{minimum\ torque} * 100 \qquad Equation\ 3.13$$

$$Plastic\ viscosity\ relative\ error(\%) = \frac{apparent\ viscosity - plastic\ viscosity}{apparent\ viscosity} * 100 \qquad Equation\ 3.14$$

Analyzing the results, one can notice that PPM mixtures displayed lower error values than the ACI mixtures, which means that the HB model is quite competent to describe the fresh state behaviour of PPM-mix-proportioned FRC. The latter suggests that FRC concrete might be mix-designed to present targeted ranges of yield stress and plastic viscosity for distinct applications through the HB model.

3.7.4 HARDENED STATE PERFORMANCE

It is well established that the compressive strength of conventional concrete is directly related to the water-to-cement ratio (Abram's law), which sets the porosity of the hydrated system. Yet, John et al. (Bruno Luís Damineli & John,

2012) verified that Abrams law does not apply to concrete mixtures proportioned with moderate to high amounts of inert fillers. In this research, advanced PPM design techniques were used to mix proportion distinct FRC mixtures with a reduced amount of PC (and moderate to high amounts of inert fillers) and compared to conventional FRC mixtures designed through the ACI method. The water-to-cement ratio was kept constant in both mix design approaches for an effective comparison of their mechanical properties. Analyzing the results obtained, one notices that the compressive strength of PPM designed mixtures was higher (i.e. 47%, on average) than ACI designed mixes. The latter seems to demonstrate that although Abrams law is still the most critical factor controlling the compressive strength of conventional concrete mixtures, advanced mix-design techniques (i.e. PPMs in this work) characterized by a theoretical improved packing density of granular systems may further enhance the mechanical performance of concrete mixtures, especially with moderate to low amounts of PC and incorporating inert fillers. Fibers are not supposed (nor used) to influence or enhance the compressive strength of cementitious systems. Yet, an improper proportioning and/or compaction of FRC mixes may lead to systems with worse microstructure (i.e. porosity) than conventional concrete, which in turn may lower the compressive strength of systems with fiber. Conversely, confinement effects enhancing performance were also highlighted by (Abbass et al., 2018). These effects might explain, at least partially, along with the mix-proportioning approach (i.e. PPM vs ACI) the compressive strength variations obtained in this work.

FRC mixtures proportioned through PPMs displayed similar or superior results of flexural strength when compared to ACI mixtures. This is a very important output since flexural strength results indicate the ability of a given mixture to control first cracking and crack propagation. Available empirical relations between the compressive strength and flexural strength are given in Table 3.10 (ACI 318R, 2014; Ince, Erdem, Derogar, & Yuzer, 2015; Shah & Ahmad, 1985; Xu & Shi, 2009).

Table 2.10 Published empirical relations between compressive strength and flexural strength.

ACI 318-14	Ahmed and Shah	Xu and Shi	Perumal
$ft = 0.62fc^{0.5}$	$ft = 0.44fc^{0.5}$	$ft = 0.39fc^{0.59}$	$ft = 0.259fc^{0.843}$

Figure 3.12 displays the relative error Equation 3.15 between the obtained experimental results and available empirical relations.

$$Flexural\ strength\ relative\ error(\%) = \frac{MOR - ft}{MOR} * 100 \qquad Equation\ 3.15$$

Where MOR is the experimental flexural strength (MOR) result obtained in this study, and ft is the empirical obtained flexural strength value according to the exmpirical relations in Table 3.8.

The obtained experimental results deviate from the empirical relations, where most of the flexural strength results are underestimated (positive relative error) by the available empirical relations developed by (ACI 318R, 2014; Shah & Ahmad, 1985; Xu & Shi, 2009), which was more pronounced in the case of the ACI mixtures.

In the case of the PPM mixtures, the underestimation of the obtained experimental results from the empirical relations may be attributed to the fact that they are developed for conventionally designed FRC, whereas the mix design approach adopted in this study (i.e. PPMs) and the dilution effect of IF may have led to an effective dispersion of fibers in the mixtures and increased the experimental flexural strength.

On the other hand, the deviation from the obtained flexural strength results of the ACI mixtures may be related to the fact that the developed relations were developed for straight, and hooked-end fibers, whereas the fibers used in this study presents a wavy profile, which may have produced an increase in the experimental flexural strength results when compared to the empirical obtained values.

In addition, it can be noticed that the range of error is higher in the case of the ACI mixtures. This impact may be related to the fact that the developed empirical relations only account for compressive strength of the mixtures; however, it was shown that flexural strength results obtained in this work generally increased as fiber content/and or length increased, whereas the compressive strength remained similar in most cases regardless of fiber content/and or length. Finally, it can be noticed that the experimental results of the PPM mixtures were overestimated by the empirical relation between compressive strength and flexural strength developed by (Perumal, 2015), which may be attributed to the fact that the latter was developed for high-strength FRC (i.e. compressive strength > 45 MPa).

An enhancement was noticed in the toughness as a function of the fiber content/and or length. This impact is attributed due to the confinement effect of fibers at high content which in turn provides the FRC with an enhanced crack-growth arrest mechanism. Furthermore, the PPM mixtures with PP fibers exhibited higher toughness values than mixtures with S fibers, which may be related to the higher aspect ratio of the PP fibers and resulted in an increase in the total amount of fibers in the mixture at a fixed fiber content, improving the crack-growth arrest mechanism. In addition, higher toughness values were noticed for PPM mixtures with a higher amount of inert fillers (i.e. q-factor 0.21). This

impact may be attributed to an effective uniform dispersion of fibers in the mixtures caused by the diluting effect of limestone fillers, which also noted by (Cao, Ming, He, Li, & Shen, 2019). Finally, it is worth mentioning that all PPM mixtures exhibited improved load-deflection behaviour when compared to the ACI mixtures, where in some cases the PPM mixture exhibited pseudo-deflection hardening behaviour. The pseudo-deflection hardening behaviour of concrete is associated with the appearance of multiple cracks increasing in density until composite ultimate flexural load is reached, changing the failure mode from quasi-brittle to ductile (Z. Li, 2011). The latter may be attributed to the mix design approach adopted (i.e. PPMs) characterized by a theoretical increased packing density, accompanied by the dilution effect of inert fillers which have improved the fiber dispersion efficiency and ultimately the concrete load-deflection behaviour. This performance was similar to the load-deflection behaviour of high performance FRC noted by Abbas et al. (2018). Furthermore, the FRC pseudo-strain hardening behaviour was also noticed in some PPM mixtures where the residual stress increased as the deflection raised. Finally, some mixtures displayed similar residual load values regardless of the fiber content; this could be related to the reinforcement efficiency at low fiber contents when subjected to low deflection values.

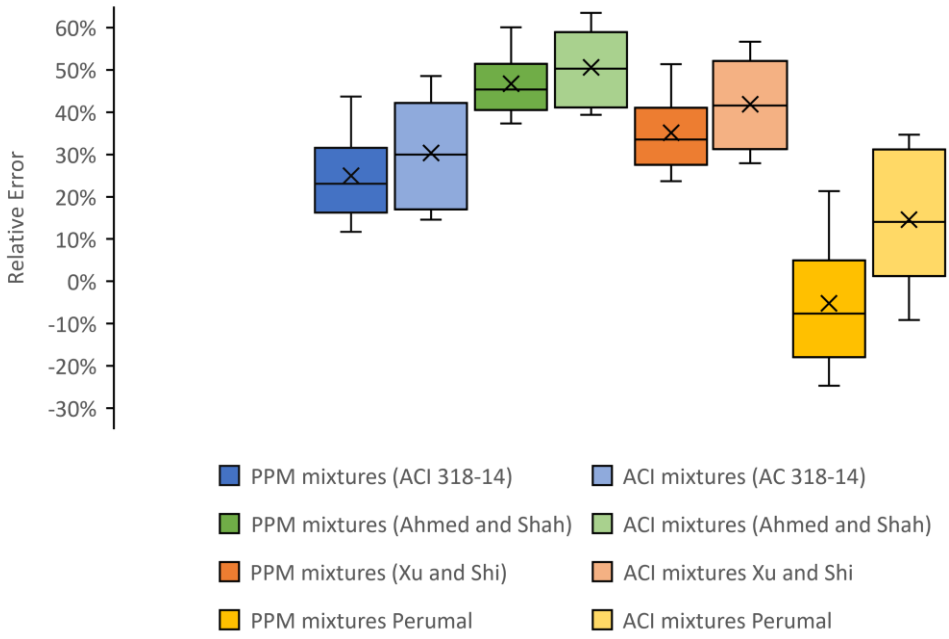

Figure 3.12 Relative error between the experimental flexural strength results and the empirical values.

3.7.5 ECO-EFFICIENCY OF FRC MIXTURES

Figure 3.13 presents a summary of international records correlating bi factors with compressive strength. The bi results obtained in this work through both PPM and ACI methods are also included in the plot for comparison purposes. Analyzing the plot below, one notices that most of the concrete produced for critical infrastructure worldwide (i.e. 20-40 MPa) is proportioned with moderate to high amounts of PC and thus yield high bi factors (i.e. 10 $kg.m^{3}.MPa^{-1}$) (Bruno L. Damineli et al., 2010). The latter is even more critical for FRC mixtures designed with conventional procedures such as ACI, where extremely high bi values of around 14.5 to 18.5 $kg.m^{3}.MPa^{-1}$ may be achieved. However, the use of advanced techniques such as continuous PPM may efficiently lower down the bi values of FRC mixtures while keeping and or enhancing performance in the fresh and hardened states; hence PPMs seem to be a suitable way to proportion eco-efficient FRC.

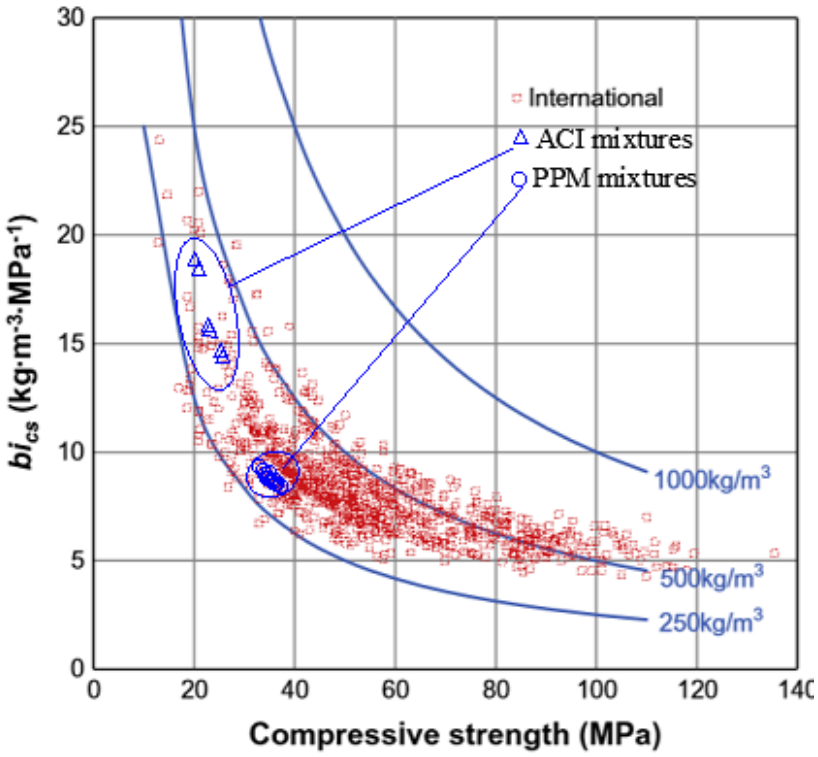

Figure 3.13 Relationship between binder intensity and compressive strength at 28-days with international records adapted from (Bruno L. Damineli et al., 2010).

3.8 CONCLUSIONS

This work studied the use of PPMs to mix-proportionFRC concrete mixtures with suitable fresh and hardened state properties along with low carbon footprint. The main outcomes of the current research are found hereafter:

- FRC mixtures designed through PPMs displayed higher minimum torque (yield stress) than ACI mixes. However, although also slightly higher, PPM mixtures presented quite compared results of AV when compared to ACI mix-proportioned mixtures. Moreover, all PPM designed FRC mixtures showed a shear thinning behaviour (i.e. decrease in viscosity as a function of time). The latter means that PPMs may be a suitable technique to proportion FRC vibrated and/or pumped concrete;
- All the PPMs proportioned mixtures presented similar orsuperior hardened performance (i.e. compressive strength and flexure strength) than ACI mixtures which suggests that not only eco-efficiency but also mechanical performance mau be achieved through PPMs;

- PPM mix proportioned FRC may be properly modelled with the use of Herschel-Bulkley model. This enables the possibility of mix-designing FRC concrete to present targeted ranges of yield stress and plastic viscosity for distinct applications.
- A new proposed fiber-matrix factor was proposed in this work. This factor enables further controlilng and predicting the fresh and hardened state behaviours of PPM mix-proportioned FRC concrete;
- The bi factors obtained for PPM mix-designd FRC mixes clearly indicate the higher eco-efficiency of this materials when compared to ACI propoerioned FRC concrete The latter opnes the door of a new area of PPM propoetioned FRC displaying lower embodied energy and suitable fresh and hardened performance.

CHAPTER FOUR: CONCLUSIONS AND RECOMMENDATIONS FOR FUTURE RESEARCH

4.1 CONCLUSIONS

There is currently a misconception in the concrete industry that the amount of Portland Cement (PC) is directly proportional to the material's strength. Furthermore, PC is the most expensive concrete ingredient and is responsible for the majority of CO^2 emissions generating from the construction industry. Numerous strategies are being studied over the last decades to decrease PC content and thus the environmental impact of concrete. Among these, the use of advanced mix design techniques such as particle packing models (PPMs) along with inert fillers showed promising results, specially when the former is combined with mobility parameters (MP) to control the fresh and hardened state behaviour of concrete mixtures.

In this research, low cement FRC mixtures were proportioned through advanced mix design techniques (i.e. PPMs – chapter 3) and evaluated in the fresh (i.e. VeBe time, slump, and rheological behaviour) and hardened (i.e. compressive strength, and flexural behaviour) states and compared to control FRC mixtures mix proportioned through conventional methods (i.e. ACI- absolute volume method). Chapter 3 shows the evaluation of 12 distinct eco-efficient FRC mixtures proportioned through the use of PPMs (i.e. Alfred model- using 2 q factors) and presenting PC contents of 300 kg/m^3 and compared to six conventional FRC mixtures proportioned through the ACI absolute volume method presenting PC contents of 375 kg/m^3. The main objective was to design eco-efficient mixes without compromising the material's fresh and hardened state. The main findings of this research program are as follows:

- Eco-efficiency

  Although literature shows that very few FRC mixtures are produced with PC contents lower than 400 kg/m^3, this research program proved that it is possible to produce FRC mixtures with reduced amount of PC and suitable fresh and hardened state properties. All PPMs FRC mixtures developed throughout this project can be considered as eco-efficient since the bi factors obtained was always lower than 10kg/m^3.MPa^{-1}, whereas all conventional FRC mixtures can be considered as inefficient since the bi factors obtained from all of them were higher than 10kg/m^3.MPa^{-1}.

- VeBe time and slump

The results demonstrated that PPMs can be used to produce low cement FRC mixtures with similar VeBe time trends to the conventional ACI mixtures, where flowability decreases as fiber content/and or length is increased. However, all ACI mixtures showed lower VeBe times than their companion PPM mixtures, which is very likely due to the high amounts of PC (i.e. lubrication) in these mixtures, and the lack of inert fillers (IF) which in turn may have reduced their viscosity. Similarly, the slump test results were in conjunction with the VeBe time results.

- Rheological behaviour

The results obtained in this research showed that all FRC mixtures designed through PPMs presented a shear thinning behaviour (i.e. decrease of viscosity as a function of the torque applied) regardless of fiber type, content, length or q-factor. Shear thinning behaviour brings advantages to FRC mixtures on both ends of the spectrum, where at low torque levels (i.e. casting on a gradient, or slopes) the mixtures would show resistance to slip, and reduction on bleeding and settlement. Otherwise, at high torque levels (i.e. pumped and or vibrated FRC) the mixtures flow almost freely into the formwork. Similar behaviour was noticed for most ACI control mixtures.

- Compressive strength

The results demonstrated that the amount of PC does not directly influence the compressive strength of low cement FRC mixtures. Moreover, it has been found the sole use of Abrams law is not enough to forecast the mechanical properties of FRC mixtures proportioned through PPMs. Furthermore, all PPM mixtures presented on average 47% higher compressive strength values than ACI designed mixtures. Although the latter contained 25% higher PC contents.

- Flexural Strength

The results showed that low cement FRC mixtures proportioned through PPMs exhibited similar or improved flexural behaviour when compared to conventional FRC mixtures. Furthermore, the higher the amounts of inert fillers, the higher the toughness, owing to the dilution effect of fillers which result in an effective uniform dispersion of fibers. Finally, concrete hardening behaviour was exhibited by PPM mixtures containing long

fibers (50 mm) at high fiber content. whereas other mixtures displayed concrete softening behaviour where load drops beyond the initiation of the first crack, followed by a period of recovery until an optimum point is reached, followed by a load-deflection descending curve up to failure.

- Fiber-Matrix factor

  A new factor is proposed (Fiber-Matrix factor) that considers the different variables that the FRC mixture could present, such as the Interparticle Separation Distance (IPS), Maximum Paste Thickness (MPT), Fiber content, and Fiber aspect ratio. Results show that this factor strongly correlates with the VeBe time, and toughness of the mixtures. whereas the fiber-matrix factor increases, interparticle spacing is increased, and fiber factor decreases, which results in higher flowability, and lower toughness values.

4.2 RECOMMENDATIONS FOR FUTURE RESEARCH

The main objective when developing/studying new materials is to promote their utilization into the building industry. Furthermore, it is also intended to further improve the available knowledge, so that new materials could be covered within the scope of design guidelines and recommendations. Regarding these aspects, the use of PPM to mix-design low cement FRC in this research has been limited to the fresh state, and short-term mechanical response. Therefore, further investigations can be drafted, as presented hereafter:

- Single fiber pull-out testing, and microscopic analysis must be performed on low cement FRC mixtures with distinct mix-proportions to understand the mechanism of failure of high-density low cement FRC systems and how they differ from conventional FRC. Moreover, the porosity of low embodied energy FRC systems mix proportioned through PPMs must be evaluated and compared to conventional FRC systems.
- An in-depth evaluation on the behaviour of low cement FRC systems during their service life should be performed. Hence, research on durability, shrinkage, fire resistance and fatigue properties of eco-efficient FRC is recommended.
- Development of empirical/analytical relations between the rheology of fresh low cement FRC, mobility parameters, and the FMF. Moreover, an investigation on the orientation of fibers in low cement FRC systems during flow for different casting procedures must be performed and how they differ from conventional FRC systems.

- The use of moderate to high amounts of inert fillers and their effect on the fresh, hardened states, and long-term behaviour of low cement FRC systems is still limited and should be further evaluated.
- Appraisal of the structural behaviour of low cement FRC systems under shear, and/or cyclic loadings should be performed. Finally, an assessment of eco-efficient FRC systems behaviour on large scale elements is recommended.

4.3 REFERENCES

Abbass, W., Khan, M. I., & Mourad, S. (2018). Evaluation of mechanical properties of steel fiber reinforced concrete with different strengths of concrete. *Construction and Building Materials*, *168*, 556–569. https://doi.org/10.1016/j.conbuildmat.2018.02.164

Abdallah, S., Fan, M., & Rees, D. W. A. (2018). Bonding Mechanisms and Strength of Steel Fiber – Reinforced Cementitious Composites : Overview Bonding Mechanisms and Strength of Steel Fiber – Reinforced Cementitious Composites : Overview, (March). https://doi.org/10.1061/(ASCE)MT.1943-5533.0002154

ACI 318R. (2014). *ACI 318R-14 - Building Code Requirements for Structural Concrete*. *American Concrete Institute*.

ACI 544. (1999). ACI 544.4R-88: Design Considerations for Steel Fiber Reinforced Concrete. *ACI Committee 544*, *88*(Reapproved), 18.

ACI Comittee 544. (2014). *Guide for Specifying, Proportioning, Mixing, Placing, and Finishing Steel Fiber Reinforced Concrete*. *ACI Materials Journal* (Vol. 90). https://doi.org/10.14359/4046

ACI Comittee 544. (2017). *Report on the Measurement of Fresh State Properties and Fiber Dispersion of Fiber-Reinforced Concrete*.

ACI Committee 211. (2004). *Standard Practice for Selecting Proportions for Normal Heavyweight , and Mass Concrete (ACI 211 . 1-91) Reapproved 2002*.

ACI Committee 544. (2008). *Guide for Specifying , Proportioning , and Production of Fiber-Reinforced Concrete*.

Andreasen, A. H. M. (1930). Ueber die Beziehung zwischen Kornabstufung und Zwischenraum in Produkten aus losen Körnern (mit einigen Experimenten). *Kolloid-Zeitschrift*, *50*(3), 217–228. https://doi.org/10.1007/BF01422986

Andrew, R. M. (2017). Global CO2 emissions from cement production. *Earth System Science Data Discussions*, 1–52. https://doi.org/10.5194/essd-2017-77

ASTM C143. (2015). Standard Test Method for Slump of Hydraulic-Cement Concrete. *Astm C143*, (1), 1–4. https://doi.org/10.1520/C0143

ASTM C1609. (2012). *Standard Test Method for Flexural Perfromance of Fiber-Reinforced Concrete (Using Beam with Third-point Loading)*. https://doi.org/10.1520/C1609

ASTM International. (2015a). C39/C39M-15a: Standard Test Method for Compressive Strength of Cylindrical Concrete Specimens. *American Society for Testing and Materials*, 1–7. https://doi.org/10.1520/C0039

ASTM International. (2015b). *Standard Test Method for Relative Density (Specific Gravity) and Absorption of Fine*. https://doi.org/10.1520/C0128-15.2

ASTM International. (2015c). *Standard Test Method for Relative Density (Specific Gravity) and Absorption of Coarse Aggregate*. *ASTM - C127-15*. https://doi.org/10.1520/C0127-15.2

ASTM International. (2016). *ASTM C192/C192M-16a: Standard Practice for Making and Curing Test Specimens in the Laboratory*. https://doi.org/10.1520/C0192

ASTM International. (2017). *Standard Practice for Sampling Freshly Mixed Concrete*. *ASTM - C172/C172M-17*. https://doi.org/10.1520/C0172

ASTM International. (2018). *Standard Specification for Concrete Aggregates*. https://doi.org/10.1520/C0033

Banthia, N. (2009). Fiber reinforced concrete for sustainable and intelligent infra structure. *… on Sustainable Built Environment Infrastructures in …*, (October), 337–350. Retrieved from http://www.researchgate.net/publication/228846983_Fiber_reinforced_concrete_for_sustainable_and_intelligent_infrastructure/file/72e7e5294b7eb46534.pdf

Banthia, Nemkumar, Bindiganavile, V., Jones, J., & Novak, J. (2014). Fiber-reinforced concrete in precast concrete applications: Research leads to innovative products. *PCI Journal*, *57*(3), 33–46. https://doi.org/10.15554/pcij.06012012.33.46

Banthia, Nemkumar, Zanotti, C., & Sappakittipakorn, M. (2014). Sustainable fiber reinforced concrete for repair applications. *Construction and Building Materials*, *67*(PART C), 405–412. https://doi.org/10.1016/j.conbuildmat.2013.12.073

Beaupre, D. (1994). *Rheology of High Performance Shotcrete*. *Therapiewoche*. University Of British Columbia.

Bentur, A., & Sidney, M. (2007). *Fibre Reinforced Cementitious Composites*. *Composites* (2nd Editio). Taylor& Francis Group. https://doi.org/10.1016/0010-4361(79)90446-4

Berodier, E., & Scrivener, K. (2014). Understanding the filler effect on the nucleation and growth of C-S-H. *Journal of the American Ceramic Society*, *97*(12), 3764–3773. https://doi.org/10.1111/jace.13177

British Standards Institution. (2009). *Testing fresh concrete - Vebe test*. Retrieved from https://bsol.bsigroup.com/Home

Canadian Standard Association. (2018). *Cementitious materials for use in concrete.* (5th ed.). Canadian Standard

Association.

Cao, M., Ming, X., He, K., Li, L., & Shen, S. (2019). Effect of Macro-, Micro- and Nano-Calcium Carbonate on Properties of Cementitious Composites—A Review. https://doi.org/10.3390/ma12050781

Cunha, V. M. C. F. (2014). *Steel Fibre Reinforced Self-Compacting Concrete (from Micro-Mechanics to Steel Fibre Reinforced Self-Compacting Concrete (from Micro-Mechanics to Composite Behaviour)*.

Dadsetan, S., Grazia, M. T. De, & Sanchez, L. (2017). The use of low cement structural concrete as a sustainable alternative for civil industry, (October).

Damineli, Bruno L., John, V. M., Lagerblad, B., & Pileggi, R. G. (2016). Viscosity prediction of cement-filler suspensions using interference model: A route for binder efficiency enhancement. *Cement and Concrete Research*, *84*, 8–19. https://doi.org/10.1016/j.cemconres.2016.02.012

Damineli, Bruno L., Kemeid, F. M., Aguiar, P. S., & John, V. M. (2010). Measuring the eco-efficiency of cement use. *Cement and Concrete Composites*, *32*(8), 555–562. https://doi.org/10.1016/j.cemconcomp.2010.07.009

Damineli, Bruno Luís, & John, V. M. (2012). Developing Low CO2 Concretes: Is Clinker Replacement Sufficient? The Need of Cement Use Efficiency Improvement. *Key Engineering Materials*, *517*, 342–351. https://doi.org/10.4028/www.scientific.net/kem.517.342

de larrard, F. (1999). *Concrete Mixture Proportioning*.

de Oliveira, Ivone R.; Studart, A. R., Pileggi, R. G., & Pandolfelli, V. C. (2000). *Dispersão e Empacotamento de Partículas - Princípios e Aplicações em Processamento Cerâmico*.

Fennis, S. A. A. M., & Walraven, J. C. (2012). Using particle packing technology for sustainable concrete mixture design. *Heron*, *57*(2), 73–101.

Ferrara, L., Park, Y. D., & Shah, S. P. (2007). A method for mix-design of fiber-reinforced self-compacting concrete. *Cement and Concrete Research*, *37*(6), 957–971. https://doi.org/10.1016/j.cemconres.2007.03.014

Figueiredo, A. D. de, & Ceccato, M. R. (2015). Workability Analysis of Steel Fiber Reinforced Concrete Using Slump and Ve-Be Test. *Materials Research*, *18*(6), 1284–1290. https://doi.org/10.1590/1516-1439.022915

Fuller, W.B.; Thompson, S. E. (1907). THE LAWS OF PROPORTIONING CONCRETE. *TRANSACTIONS OF THE AMERICAN SOCIETY OF CIVIL ENGINEERS*, 67–143.

Funk, J. E., & Dinger, D. R. (1994). *Predictive Process Control of Crowded Particulate Suspensions*. *Predictive Process Control of Crowded Particulate Suspensions*. https://doi.org/10.1007/978-1-4615-3118-0

G. Krage, O. H. W. (2007). Rheology of synthetic-fiber reinforced SCC. In *5th International RILEM Symposium on Self-Compacting Concrete*.

Granju, J., & Balouch, S. U. (2005). Corrosion of steel fibre reinforced concrete from the cracks, *35*, 572–577. https://doi.org/10.1016/j.cemconres.2004.06.032

Grazia, M. T. De. (2018). Contribution to the understanding of fresh and hardened state properties of low cement concrete.

Grunewald, S. (2004). *Performance-based design of self-compacting fibre reinforced concrete*. *Technology*. https://doi.org/uuid:07a817aa-cba1-4c93-bbed-40a5645cf0f1

Grünewald, S. (2011). *Fibre reinforcement and the rheology of concrete*. *Understanding the Rheology of Concrete*. Woodhead Publishing Limited. https://doi.org/10.1016/B978-0-85709-028-7.50009-1

Guerini, V., Conforti, A., Plizzari, G., & Kawashima, S. (2018). Influence of Steel and Macro-Synthetic Fibers on Concrete Properties. *Fibers*, *6*(3), 47. https://doi.org/10.3390/fib6030047

Ince, C., Erdem, B. Z., Derogar, S., & Yuzer, N. (2015). The Effects of SCMs on the Mechanical Properties and Durability of Fibre Cement Plates, *9*(8), 893–899.

Innocentini, M. D. M., Pileggi, R. G., Ramal, F. T., & Pandolfelli, V. C. (2003). PSD-Designed refractory castables. *American Ceramic Society Bulletin*, *82*(7), 9401-9406.

Johnston, C. D. (1984). Measures of the Workability of Steel Fiber Reinforced Concrete and Their Precision. *Cement, Concrete and Aggregates*, *6*(2), 74–83.

Kawashima, S. et al. (2012). Study of the mechanisms underlying the fresh-state response of cementitious materials modified with nanoclays.

Knop, Y., & Peled, A. (2016). Packing density modeling of blended cement with limestone having different particle sizes. *Construction and Building Materials*. https://doi.org/10.1016/j.conbuildmat.2015.09.063

Komastka, S. H., Kerkhoff, B., & Panarese, W. C. (2003). *Design and Control of Concrete Mixtures. Construction*. https://doi.org/2001007603

Kuder, K. G., Ozyurt, N., Mu, E. B., & Shah, S. P. (2007). Rheology of fiber-reinforced cementitious materials, *37*, 191–199. https://doi.org/10.1016/j.cemconres.2006.10.015

Kumar, S. V., & Santhanam, M. (2003). Particle packing theories and their application in concrete mixture proportioning: A review. *Indian Concrete Journal*, *77*(9), 1324–1331.

Labib, W. A. (2018). Fibre Reinforced Cement Composites. In *Cement based materials*. https://doi.org/10.5772/intechopen.75102

Larrard, F. De, Ferraris, C. F., & Sedran, T. (1998). Fresh concrete : A HerscheI-Bulkley material, *31*(September), 494–498.

Laskar, A. I., & Talukdar, S. (2008). Rheology of steel fiber reinforced concrete. *Civil Engineering*, *9*(2), 167–177.

Leung, H. Y., & Balendran, R. V. (2003). Properties of fresh polypropylene fibre reinforced concrete under the influence of pozzolans. *Journal of Civil Engineering and Management*, *9*(4), 271–279. https://doi.org/10.1080/13923730.2003.10531339

Li, V. C. (2019). *Engineered Cementitious Composites (ECC)*. *Journal of Advanced Concrete Technology* (Vol. 1). Springer-Verlag GmbH Germany, part of Springer Nature 2019. https://doi.org/10.3151/jact.1.215

Li, Z. (2011). *Advanced Concrete Technology*. https://doi.org/10.1002/9780470950067

Mangulkar, M., & Jamkar, S. (2013). Review of Particle Packing Theories Used For Concrete Mix Proportioning. *International Journal Of Scientific & Engineering Research*, *4*(5), 143–148. Retrieved from http://www.ijser.org/researchpaper%5CReview-of-Particle-Packing-Theories-Used-For-Concrete-Mix-Proportioning.pdf%5Cnhttp://www.ijser.org/researchpaper/Review-of-Particle-Packing-Theories-Used-For-Concrete-Mix-Proportioning.pdf

Milewski, J. V. (1973). A study of the packing of milled fibreglass and glass beads. *Composites*, *4*(6), 258–265. https://doi.org/10.1016/0010-4361(73)90392-3

Moghimi, G. (2014). *Behavior of Steel-Polypropylene Hybrid Fiber Reinforced Concrete*.

Naaman, A. E. (2003). Engineered Steel Fibers with Optimal Properties for Reinforcement of Cement Composites, *1*(3), 241–252.

Neville, A. M. M., & Brooks, J. J. J. (2010). *Concrete Technology Second Edition*. *Building and Environment*. https://doi.org/10.1016/0360-1323(76)90009-3

Ortega, F. S. ., Pileggi, R. G., Studart, A. R., & Pandolfelli, V. C. (2002). IPS A Viscosity - Predictive Parameter. *American Ceramic Society Bulletin*, 44–52.

Perumal, R. (2015). Correlation of compressive strength and other engineering properties of high-performance steel fiber-reinforced concrete. *Journal of Materials in Civil Engineering*, *27*(1), 1–8. https://doi.org/10.1061/(ASCE)MT.1943-5533.0001050

Pileggi, R. G., Alferes Filho, R. S., Motezuki, F. K., Romano, R. C. O., & Figueiredo, A. D. (2016). Evaluating the applicability of rheometry in steel fiber reinforced self-compacting concretes. *Revista IBRACON de Estruturas e Materiais*, *9*(6), 969–988. https://doi.org/10.1590/s1983-41952016000600008

Raman, S. N., Jumaat, M. Z., Bin Mahmud, H., & Zain, M. F. M. (2007). Fibre reinforced concrete and high performance fibre reinforced cementitious composites: An overview. *Jurutera*, (July), 32–35.

Shah, S. P., & Ahmad, S. H. (1985). Structural Properties of High Strength Concrete and Its Implications for Precast Prestressed Concrete. *Journal - Prestressed Concrete Institute*, *30*(6), 92–119.

https://doi.org/10.15554/pcij.11011985.92.119

Steven H. Kosmatka, Beatrix Kerkhoff, and W. C. P. (2002). *Design and Control of Concrete Mixtures*. (Portland Cement Association, Ed.) (14th Editi).

T. de Grazia, M., F. M. Sanchez, L., C. O. Romano, R., & G. Pileggi, R. (2019). Investigation of the use of continuous particle packing models (PPMs) on the fresh and hardened properties of low-cement concrete (LCC) systems. *Construction and Building Materials*, *195*, 524–536. https://doi.org/10.1016/j.conbuildmat.2018.11.051

Tattersall, G. H. (1976). The workability of concrete, A Viewpoint Publication. *Cement and Concrete Association*.

Varhen, C., Dilonardo, I., de Oliveira Romano, R. C., Pileggi, R. G., & de Figueiredo, A. D. (2016). Effect of the substitution of cement by limestone filler on the rheological behaviour and shrinkage of microconcretes. *Construction and Building Materials*, *125*, 375–386. https://doi.org/10.1016/j.conbuildmat.2016.08.062

Vogt, C. (2010). Ultrafine particles in concrete - Influence of ultrafine particles on concrete properties and application to concrete mix design. *School of Architecture and the Built Environment Division of Concrete Structures, PhD*, 177.

Wafa, F. F. (1990). Properties and Applications of Fiber Reinforced Concrete. *JKAU: Eng. Sci*, *2*(September), 49–63. https://doi.org/10.4197/Eng.2-1.4

Wedding, P., Balaguru, P., & Ramakrishnan, V. (2010). Comparison of Slump Cone and V-B Tests as Measures of Workability for Fiber-Reinforced and Plain Concrete. *Cement, Concrete and Aggregates*, *9*(1), 3. https://doi.org/10.1520/cca10400j

Xu, B. W., & Shi, H. S. (2009). Correlations among mechanical properties of steel fiber reinforced concrete. *Construction and Building Materials*, *23*(12), 3468–3474. https://doi.org/10.1016/j.conbuildmat.2009.08.017

Yazici, Ş., Inan, G., & Tabak, V. (2007). Effect of aspect ratio and volume fraction of steel fiber on the mechanical properties of SFRC. *Construction and Building Materials*, *21*(6), 1250–1253. https://doi.org/10.1016/j.conbuildmat.2006.05.025

Yousuf, S., Sanchez, L. F. M., & Shammeh, S. A. (2019). The use of particle packing models (PPMs) to design structural low cement concrete as an alternative for construction industry. *Journal of Building Engineering*, *25*(October 2018), 100815. https://doi.org/10.1016/j.jobe.2019.100815

Yu, A. -B, Standish, N., & McLean, A. (1993). Porosity Calculation of Binary Mixtures of Nonspherical Particles. *Journal of the American Ceramic Society*, *76*(11), 2813–2816. https://doi.org/10.1111/j.1151-2916.1993.tb04021.x

Yu, A. B., & Standish, N. (1993). Characterisation of non-spherical particles from their packing behaviour, *74*, 205–213.

Yu, R., Spiesz, P., & Brouwers, H. J. H. (2015). Development of an eco-friendly Ultra-High Performance Concrete (UHPC) with efficient cement and mineral admixtures uses. *Cement and Concrete Composites*, *55*, 383–394. https://doi.org/10.1016/j.cemconcomp.2014.09.024

Yu, Rui, Song, Q., Wang, X., Zhang, Z., Shui, Z., & Brouwers, H. J. H. (2017). Sustainable development of Ultra-High Performance Fibre Reinforced Concrete (UHPFRC): Towards to an optimized concrete matrix and efficient fibre application. *Journal of Cleaner Production*, *162*, 220–233. https://doi.org/10.1016/j.jclepro.2017.06.017

Yu, Rui, Spiesz, P., & Brouwers, H. J. H. (2012). A method for calculating equivalent diameter of fiber in Self-Compacting Fiber Reinforced Concrete. *Proceedings of the 18th International Conference on Building Materials (Ibausil), Weimar*. Retrieved from http://josbrouwers.bwk.tue.nl/publications/Conference87.pdf

APPENDIX

A1 SAMPLE OF CALCULATION

In this section, an example of mix-proportions using continuous PPMs (i.e. Alfred model) is performed to systematically illustrate the steps of this procedure. For the sake of this example, the mixture *PPM-S1.0-50-0.26* is selected.

First, the q-factor is selected according to the required fresh state performance. In this example, a q-factor of 0.26 was selected aiming for a vibrated FRC mix. It is worth noting that q factors raging from 0.20-0.22 are normally selected for self-consolidating concrete (SCC), while q factors varying from 0.33-0.37 are used for roller compacted (RCC) or no-slump concrete. Q factors from 0.24-0.28 are often used for vibrated and/or pumped mixtures.

The minimum particle size selected was 0.5 μm to match the PSD of the cement and limestone filler used, while the largest particle size selected was 19000 μm. The cumaltive percentage finer than (CPFT) is then calculated through the Alfred's model given previously by Equation 3.3, Where:

$$CPFT = \left(\frac{d^q - d_{min}^q}{D_{max}^q - d_{min}^q}\right) x\ 100$$

Table 5.1 and Figure 5.1 display the cumulative and discrete volumetric passing percentages of each particle size in columns (1) and (2), respectively

Table 5.1 grading of aggregates and fines for mixture PPM-S1.0-50-0.26.

	Original grading with no gaps		Normalized discrete grading
Particle size (μm)	(1) CPFT	(2) Discrete passing %	(3) Discrete Passing %
0.5	0%	9.79%	9.79%
15	10%	3.29%	3.29%
30	13%	3.94%	3.94%
60	17%	3.40%	3.40%
100	20%	3.04%	0.00%
150	23%	5.99%	6.23%
300	29%	7.18%	7.46%
600	37%	8.37%	8.70%
1180	45%	10.25%	10.66%
2360	55%	12.40%	12.89%
4750	68%	14.72%	15.30%
9500	82%	6.60%	6.86%
12500	89%	11.03%	11.46%
19000	100%	0.00%	0.00%

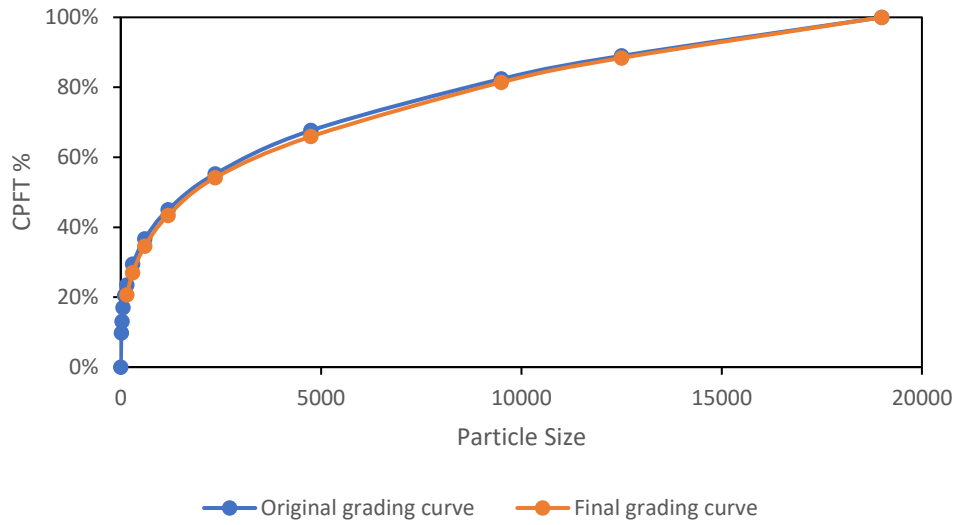

Figure 5.1 CPFT versus particle size for mixture PPM-S1.0-50-0.26.

The second step is to select the amount of cement in the mixtures. ACI advise the use of a minimum content of 320 kg/m^3 for mixtures with nominal maximum size aggregates of 20 mm (Komastka et al., 2003). For the purpose of reducing the carbon footprint of these mixtures and comparing them with the ACI control mixtures, the cement content selected was 300 kg/m^3.

The third step is to define the water-to-cement (w/c) ratio, which is usually selected in Canada to meet anticipated and aggressive exposure conditions. However in this work, a w/c of 0.64 was selected to proportion conventional concrete mixtures of about 25 MPa, presenting enhanced flowability in the frest state, so that comparisons amongst distinct mix-design techniques (i.e. ACI vs PPM) and features (Vf, type of fibre, fillers, q factor, etc.) might be facilitated. The water content used was then equal to 192 Kg/m^3. Where: 0.64 (w/c) * 300 (PC content in kg/m^3).

The forth step is to define the fiber content, based on the required flexural performance. However, for long fibers (i.e. > 35 mm), a fiber content higher than 1.50 Vf% could cause entaglement and segregation during mixing, which would compromise the flexural performance of the FRC. For that purpose, an upper limit of 1.0 Vf% was defined for these mixtures.

The fifth step is to calculate the volumetric diameter (dv) of the fibers, which was calculated through Equation 2.15 and found to be 4.60 mm for the selected fibers in this example, where:

$$dv = 1.145 * \left(L/D\right)^{1/3} * D$$

Since dv is in the range between 4.75 mm and 2.36 mm, a portion of that aggregate size is removed equal to the added volume of fibers, which in this case was equal to 1.0%.

The sixth step is to calculate the amount in mass of each ingredient in the mixture by multiplying the volume with the density of the material.

The cement and fillers used in this study had a maximum size of 100 μm, and the lowest aggregate size was 150 μm. For this reason, a gap is created in the grading of the system between 150 μm and 100 μm, and the cumulative and discrete volume percentages are normalized as shown in Table 5.1, column (3).

Since the cement content was selected at 300 kg/m^3, and the dry cumulative volume of fines for particles smaller than 100 μm was 20.42% (in the first iteration), this would result in a cement content of around 445 kg/m^3; the excess amount of cement is replaced with the limestone filler in the second iteration, where the dry volumetric % of the filler added is 8.34%, and remaining dry cement volume that corresponds to 300 kg/m^3 is 12.09%.

The final mass of each ingredient in the wet FRC mixture is calculated based on its proportion to cement in the dry state, an example:

Proportion of Coarse aggregates = $\frac{928}{380.71}$ = 2.44

Mass of coarse aggregates = 300*2.44 = 732 kg/m^3. Table 5.2 displays the dry mass of each ingredient in the mixture.

Table 5.2 mix proportions of mixture PPM-S1.0-50-0.26

Material	Skeletal volume	Skeletal mass (kg/m^3)	Proportions	Final mass (kg/m^3)
Coarse aggregates	33.63%	928	2.44	732
Fine Aggregates	44.67%	1219.51	3.20	961
Cement	12.09%	380.71	1.00	300
Replacement filler	8.34%	226.10	0.59	178
Water	-	-	0.64	192
Fibers	1.27%	99.60	0.26	78.50

*Note: in the final mix proportions, an amount of 2% of entrapped air is considered in the calculations.

The final step is to perform trial batches to define the amount of chemical admixtures to facilitate flowability based on the required fresh state performance. The amount of chemical admixtures (i.e. combination of mid-range and high-range plasticizers) is usually selected to provide conventional concrete mixes with a given consistency (i.e. slump). However, vibration is always required for FRC mixtures which prevents the use of slump test; therefore the VeBe test was selected to set the "fresh performance" of the mixtures studied in this research. An upper limit of 25 seconds was then selected for all mixes. Trial batches showed that the amount of chemical admixtures required to provide all mixtures with a VeBe upper limit of 25 seconds was a combination of 0.20% mid-range plasticizer and 0.40% high-range plasticizer by mass of cement.

Figure 5.2 illustrates the consecutive steps to mix design low cement FRC using PPM.

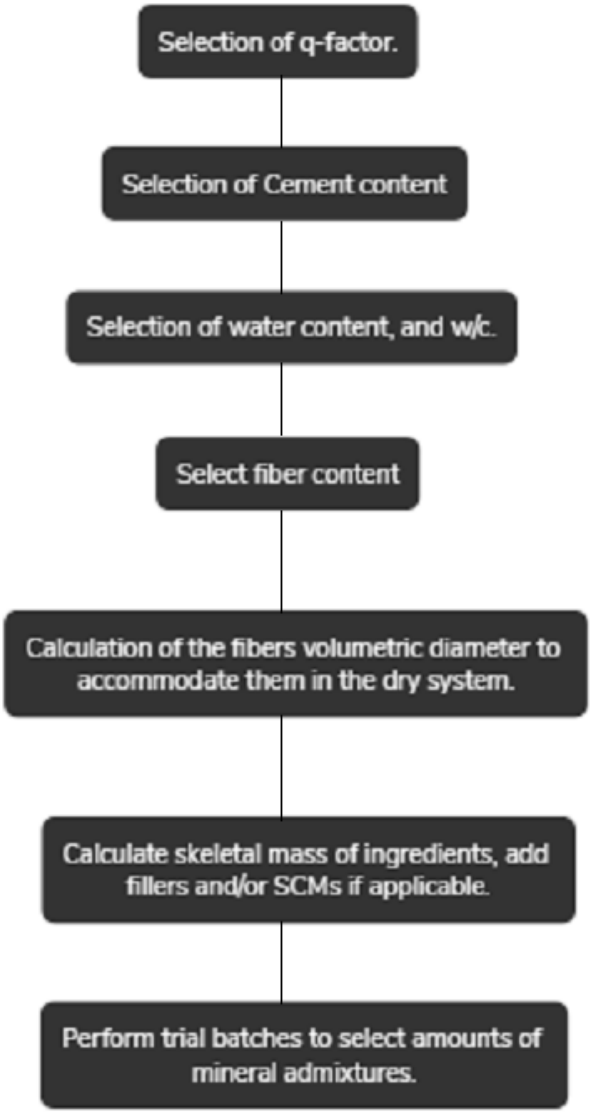

Figure 5.2 Flow chart of the mix-proportioning steps for low cement FRC using PPM.